Transversity distributions in the nucleon in the large-N_c limit

P. Schweitzer,[1] D. Urbano,[2] M. V. Polyakov,[1,3] C. Weiss,[4] P. V. Pobylitsa,[1,3] and K. Goeke[1]

[1]*Institut für Theoretische Physik II, Ruhr-Universität Bochum, D-44780 Bochum, Germany*
[2]*Faculdade de Engenharia da Universidade do Porto, 4000 Porto, Portugal*
[3]*Petersburg Nuclear Physics Institute, Gatchina, St. Petersburg 188350, Russia*
[4]*Institut für Theoretische Physik, Universität Regensburg, D-93053 Regensburg, Germany*

We compute the quark and antiquark transversity distributions in the nucleon at a low normalization point ($\mu \approx 600$ MeV) in the large-N_c limit, where the nucleon can be described as a soliton of an effective chiral theory (chiral quark-soliton model). The flavor-nonsinglet distributions $\delta u(x) - \delta d(x)$ and $\delta \bar{u}(x) - \delta \bar{d}(x)$ appear in leading order of the $1/N_c$ expansion, while the flavor-singlet distributions $\delta u(x) + \delta d(x)$ and $\delta \bar{u}(x) + \delta \bar{d}(x)$ are nonzero only in next-to-leading order. The transversity quark and antiquark distributions are found to be significantly different from the longitudinally polarized distributions $\Delta u(x) \pm \Delta d(x)$ and $\Delta \bar{u}(x) \pm \Delta \bar{d}(x)$, respectively, in contrast with the prediction of the naive nonrelativistic quark model. We show that this affects the predictions for the spin asymmetries in Drell-Yan pair production in transversely polarized pp and $p\bar{p}$ collisions.

I. INTRODUCTION

A central property of QCD is the possibility to factorize the cross sections for some hard scattering processes involving hadrons into the cross section for the partonic subprocess involving quarks and gluons, calculable within perturbative QCD, and certain functions describing the transition from hadrons to quark and gluon degrees of freedom. Of the latter only the scale dependence can be predicted from perturbative QCD; the value of the functions themselves at a low scale can only be inferred from experiment or be calculated using nonperturbative methods. In inclusive hard scattering off the nucleon [deep-inelastic scattering (DIS)], semi-inclusive particle production, and Drell-Yan pair production, the relevant characteristics of the nucleon are the so-called quark and antiquark distributions in the nucleon—functions describing the emission in the collinear direction and subsequent absorption by the nucleon of a quark or antiquark carrying a fraction x of the nucleon momentum. At the twist-2 level, helicity conservation allows for three different types of such functions [1]. The usual unpolarized and longitudinally polarized distributions $q(x)$, $\bar{q}(x)$ and $\Delta q(x)$, $\Delta \bar{q}(x)$ correspond to probabilities for emitting and absorbing a quark or antiquark of same helicity, and can be interpreted as the sum and difference of probabilities to find a quark or antiquark with longitudinal polarization parallel or antiparallel to that of the nucleon. The third kind of functions, $\delta q(x)$, $\delta \bar{q}(x)$, describe the emission and absorption of quarks and antiquarks with different helicities [2]. They can be interpreted as the probability to find a transversely polarized quark or antiquark in a transversely polarized nucleon and are therefore referred to as transversity distributions.

The crucial difference between the transversity and the "usual" distributions lies in their chirality properties. The unpolarized and longitudinally polarized distributions parametrize the chirally even parts of the quark density matrix in the nucleon (Dirac structures γ^+ and $\gamma^+ \gamma_5$, respectively).

They can therefore be measured in DIS at the leading-twist level, where the chirality of the quarks is preserved by the hard scattering process. These distributions are by now well known, with most of the information coming from QCD fits to DIS data [3–6]. In contrast, the transversity distributions describe the chirally odd part of the quark density matrix (Dirac structure $\sigma^{+\perp} \gamma_5$). Consequently, they can be measured only in hard processes where they enter together with other chirally odd objects, chirally odd distribution, or fragmentation functions. A variety of such processes—both hadron-hadron and lepton-hadron induced—are currently being considered; see Ref. [1] for a review. In hadron-hadron collisions the transversity distribution can be measured in Drell-Yan pair production with transversely polarized protons, where one combines the transversity quark and antiquark distributions in the two protons [2,7] or in polarized jet production [8,9]. In lepton-hadron scattering transversity is in principle accessible through semi-inclusive particle production, where the transversity distribution in the target is combined with a chiral-odd fragmentation function. In single-particle production one can measure the left-right asymmetries in the fragmentation of a transversely polarized quark, which are produced by T-odd fragmentation functions (Collins effect) [10–16]. In such processes there is usually a competing contribution involving a higher-twist distribution function in the target and a chiral-even fragmentation function, which makes extraction of the transversity distribution difficult. First estimates of the transversity distributions have been reported [13,17] based on the azimuthal asymmetries measured by the HERMES [18] and Spin Muon Collaboration (SMC) [19] experiments. Alternatively, one can consider semi-inclusive production of two pions, where a T-odd structure in the fragmentation function appears due to the possibility of interference between S and P waves in the hadronic final state [20]. It has also been suggested to use so-called "handedness" correlations in multiparticle production to access the transversity distributions [13].

The transversity distributions have many interesting theoretical aspects, related to general properties of QCD as well as to the structure of the nucleon. In leading order (LO), certain inequalities have been derived by Soffer [21], giving an upper bound on the transversity distribution in terms of the longitudinally polarized and unpolarized quark distributions; see also Ref. [22]. Their Q^2 evolution and generalization to next to leading order (NLO) have been discussed in Ref. [23]. Also, it has long been noted that in the nonrelativistic quark model (no spin-orbit interaction) the transversity distributions are identical to the longitudinally polarized ones. In this sense, any measurements of the transversity distribution would have implications for our understanding of the relativistic structure of the nucleon.

Recently a method has been formulated to calculate the quark and antiquark distributions in the nucleon at a low normalization point in the large-N_c limit [24,25]. In this limit the nucleon can be described as a soliton of an effective low-energy theory based on the dynamical breaking of chiral symmetry in QCD (chiral quark-soliton model) [26]. It has been shown that this fully field-theoretic description of the nucleon preserves all qualitative properties of the quark and antiquark distributions known from QCD, such as positivity conditions, sum rules, etc. The unpolarized distributions have been computed in Refs. [24,25,29]; the results are in good agreement with the well-known parametrizations of the parton distribution functions at a low input scale [4]. In particular, this approach describes well the observed violation of the Gottfried sum rule and the flavor asymmetry of the unpolarized antiquark distribution [27,29–32]. The longitudinally polarized flavor-singlet distribution calculated in this approach [27] is also in good agreement with the parametrizations of the polarized DIS data [3]. Interestingly, the large-N_c approach predicts a large flavor asymmetry of the polarized antiquark distribution [24,25,30,31], which could produce observable effects, e.g., in semi-inclusive spin asymmetries [32] and in Drell-Yan double-spin asymmetries with polarized protons [33]. Also, the flavor-nonsinglet transversity distribution has been computed in Ref. [34] and the isosinglet one in Refs. [27,28]. We also note that the chiral quark-soliton model has been successfully applied to calculate skewed (nondiagonal) parton distributions [35]. The model also describes well a large number of hadronic observables of the nucleon as well as the other octet and decuplet baryons, such as magnetic moments, electromagnetic and weak form factors, etc.; see Refs. [36,37] for a review.

In this paper we report about a comprehensive investigation of the quark and antiquark transversity distributions in the large-N_c approach of Refs. [24,25]. We calculate both the flavor-nonsinglet distribution, which appears in leading order of the $1/N_c$ expansion, and the flavor-singlet one, which is nonzero only in next-to-leading order. In Ref. [34] an approximation was used in dealing with the contribution of the Dirac continuum of quark states in the soliton; in this paper we perform a numerical calculation of the distribution functions without further approximations. This is particularly important for the antiquark transversity distribution.

The effective chiral theory used to describe the nucleon is nonrenormalizable and defined with an explicit ultraviolet cutoff. An important problem when calculating parton distributions in this approach is to ensure that none of their essential properties such as positivity, sum rules, etc., are violated by the ultraviolet regularization. For the unpolarized and polarized distributions this problem has been studied extensively in Refs. [24,25]. Here we use the methods developed there to investigate the role of the UV cutoff on the transversity distributions. It turns out that these distributions are UV finite and can eventually be computed without any cutoff. Still, in the actual calculation of the distributions one has to introduce a cutoff during the intermediate stages, and one must make sure that the finite result in the end does not depend on this intermediate regularization procedure. We explicitly address this problem here. In particular, we shall describe an interesting anomaly-type phenomenon observed in the calculation of the transversity distributions, which can be stated as the noncommutativity of the limits of infinite UV cutoff and the chiral limit (vanishing pion mass). A thorough understanding of this phenomenon is a prerequisite for a reliable calculation of the transversity distributions in the effective chiral theory.

The plan of this paper is as follows. In Sec. II we summarize the definition and important properties of the transversity distributions and the tensor charges within QCD. Section III gives a detailed exposition of the method used to calculate the transversity quark and antiquark distributions at a low normalization point. After a brief description of the effective low-energy theory and the chiral quark-soliton model of the nucleon in Sec. III A we discuss in Sec. III B the $1/N_c$ expansion of the transversity distributions and the tensor charges. The calculation of the transversity distributions—both isovector and isoscalar—in the chiral quark-soliton model is described in Sec. III C. In particular, in this section we derive expressions for these distributions in the form of sums over contributions of quark single-particle levels in the soliton field which are used in the numerical calculations. Section III D deals with the important issue of ultraviolet regularization. The dependence of the transversity distributions on the ultraviolet cutoff is studied using analytic methods (gradient expansion). In Sec. III E we describe the anomaly-type phenomenon in the tensor charge, which is both of general theoretical interest as well as of importance in the numerical calculations. The nature of this phenomenon is clarified, and an explicit expression for the anomalous difference of the sums over contributions of occupied and nonoccupied quark levels is derived. The corresponding difference for the full *x*-dependent distribution is given in the Appendix. In Sec. IV we describe the results for the transversity distributions at the low scale. In Sec. IV A we compare the results for the transversity distributions to those for the longitudinally polarized ones [38,39] at a qualitative level, considering various limiting cases of the chiral quark-soliton model which correspond to the nonrelativistic quark model or the Skyrme model. Numerical results are presented in Sec. IV B, where also a brief description of the numerical method used to evaluate the sums over quark levels is given. In Sec. IV C we demonstrate that the calculated transversity distributions satisfy the recently derived "large-N_c versions" of positivity and Soffer inequalities [40], which

impose stronger constraints on the distributions than the "usual QCD" positivity and Soffer inequalities. Finally, in Sec. V we use our results for the transversity distributions to make predictions for the double spin asymmetries in Drell-Yan pair production in polarized pp and $p\bar{p}$ scattering. In particular, we compare the asymmetries calculated from our model distributions with those obtained by assuming $\delta q(x) \equiv \Delta q(x)$, an approximation frequently made in the literature. We find that our model distributions result in significant deviations from what is obtained with that approximation, which makes us hope that BNL Relativistic Heavy Ion Collider (RHIC) measurements may be able to discriminate between the two predictions.

The transversity distributions at a low normalization point have been studied in a variety of other approaches. Model calculations of the distributions have been performed within the bag model [7] and a constituent quark model [41]. Furthermore, these distributions have been studied in the chiral quark-soliton model [27,34] and a closely related description of the nucleon as a chiral soliton of the Nambu–Jona-Lasinio model [42]. The transversity distributions have also been estimated using QCD sum rule techniques [43]. For the tensor charges of the nucleon estimates from lattice simulations [44,45] and QCD sum rules [46] are available. The tensor charges have also been calculated within the chiral quark-soliton model [47] (the relation of these results to the present calculation is discussed in Sec. IV B). The evolution (scale dependence) of the transversity distributions has been studied by a number of groups; see Refs. [48–50].

II. TRANSVERSITY DISTRIBUTIONS IN QCD

In QCD, parton distributions are defined as expectation values of certain twist-2 light-ray operators in the nucleon state. The helicity decomposition of the matrix element of a general quark bilinear in a polarized nucleon ("spin density matrix") contains three twist-2 structures, which can be identified as the unpolarized, longitudinally polarized, and transversity distribution [1]. The explicit expression for the transversity distribution is

$$\delta q_f(x) = \int \frac{dz^-}{4\pi} e^{ixP^+z^-} \langle N(P), S_\perp|$$
$$\times \bar{\psi}_f(0)\gamma^+ \gamma_5 \slashed{S}_\perp [0,z]\psi_f(z)|N(P),S_\perp\rangle_{z^+=z_\perp=0},$$
$$(2.1)$$

where ψ_f is the quark field of flavor f, z a lightlike distance ($z^\mu z_\mu = 0$), and the light-cone coordinates are defined as[1]

---

[1]It is convenient here to define the light-cone vector components using the one- rather than the three-direction. With this choice the direction of transverse polarization of the nucleon can be chosen as the three-direction, which will make the expressions in Sec. III C look more conventional.

$$z^\pm = \frac{z^0 \pm z^1}{\sqrt{2}}, \quad \mathbf{z}^\perp = (z^2, z^3). \quad (2.2)$$

Furthermore, $[0,z]$ denotes the link operator (path-ordered exponential of the gauge field) required by gauge invariance. The nucleon state in Eq. (2.1) is transversely polarized ($S_\perp^2 = -1$, $P_\mu S_\perp^\mu = 0$), and $\slashed{S}_\perp \equiv \gamma_\mu S_\perp^\mu$. In the nucleon rest frame, the components of the polarization vector are given by

$$S_\perp^\mu = (0,0,0,\lambda), \quad (2.3)$$

where $\lambda = 2S_3 = \pm 1$ and S_3 is the spin projection on the three-axis. In this frame Eq. (2.1) reduces to

$$\delta q_f(x) = -(2S_3)\int \frac{dz^0}{4\pi} e^{ixM_Nz^0}\langle N,S_3|\bar{\psi}_f(0)(\gamma^0+\gamma^1)$$
$$\times \gamma_5\gamma^3[0,z]\psi_f(z)|N,S_3\rangle|_{z^1=-z^0 \atop z_\perp=0}. \quad (2.4)$$

The operator in Eq. (2.1) is C odd, so the corresponding antiquark distribution is obtained from the expression on the right-hand side (RHS) of Eq. (2.1) by

$$\delta\bar{q}_f(x) = -\delta q_f(-x). \quad (2.5)$$

Furthermore, the light-ray operator in Eq. (2.1) is scale dependent, so that the distributions depend on the normalization point. This dependence can be described by evolution equations for the transversity distributions, which have been studied in Refs. [48–50].

The normalization integral for the distribution, Eqs. (2.1) and (2.5), is given by the so-called tensor charge of the nucleon,

$$\delta q_f \equiv \int_0^1 dx[\delta q_f(x) - \delta\bar{q}_f(x)], \quad (2.6)$$

which is defined as the matrix element of the local pseudo-tensor operator:

$$\langle N(P),S|\bar{\psi}(-i)\sigma^{\mu\nu}\gamma_5\psi|N(P),S\rangle = (P^\mu S^\nu - P^\nu S^\mu)\delta q_f. \quad (2.7)$$

In particular, in the nucleon rest frame it is given by

$$\langle N,S_3|\bar{\psi}\gamma^0\gamma^3\gamma_5\psi|N,S_3\rangle = 2M_N(2S_3)\delta q_f. \quad (2.8)$$

III. TRANSVERSITY DISTRIBUTIONS FROM THE EFFECTIVE CHIRAL THEORY

A. Nucleon as a chiral soliton

It is generally believed that in the large-N_c limit QCD becomes equivalent to a theory of mesons, with baryons emerging as solitonic excitations [51]. While this connection alone has many interesting qualitative implications, it is not known at present how to derive this effective theory from QCD in full generality. However, quantitative calculations within the large-N_c ideology can be done in certain limiting cases where the dynamics of QCD simplifies. It is known

that at energies far below the mass of mesonic resonances (say, the rho meson) the dynamics of strong interactions is governed by the spontaneous breaking of chiral symmetry. In fact, in the long-wavelength limit the dynamics is completely described by the chiral Lagrangian containing only the Goldstone boson (pion) field to some given order in derivatives. To describe the nucleon as a chiral soliton, however, one needs an effective theory valid in a wider region of momenta. Such a theory has been derived within the framework of the instanton description of the QCD vacuum, which provides a "microscopic" picture of the dynamical breaking of chiral symmetry in QCD [52]. In this approach the effective action for the pion field is obtained in the form of an integral over quark fields, which have obtained a dynamical mass in the spontaneous breaking of chiral symmetry and which interact with the pion field in a chirally invariant way [52,53]:

$$\exp(iS_{\text{eff}}[U(x)]) = \int D\psi\, D\bar{\psi}\, \exp\left[i \int d^4x\, \bar{\psi}(i\partial\!\!\!/\right.$$

$$\left. - MU^{\gamma_5})\psi\right]. \tag{3.1}$$

Here, $\bar{\psi}, \psi$ are the fermion fields, M is the dynamical quark mass, and the Goldstone boson field is parametrized as a unitary matrix $U(x)$, with

$$U^{\gamma_5}(x) = \frac{1+\gamma_5}{2}U(x) + \frac{1-\gamma_5}{2}U^{\dagger}(x). \tag{3.2}$$

In the long-wavelength limit, when expanding in derivatives of the pion field, the effective action, Eq. (3.1), reproduces the chiral Lagrangian with correct coefficients, including the Gasser-Leutwyler $O(p^4)$ terms and the Wess-Zumino term. However, the validity of the theory defined by Eq. (3.1) is not restricted to the long-wavelength limit.

In the effective theory derived from the instanton vacuum the dynamical quark mass in Eq. (3.1) is momentum-dependent and drops to zero for momenta of the order of the inverse average instanton size, $\bar{\rho}^{-1} \simeq 600$ MeV. This provides for a natural ultraviolet cutoff of the effective theory. In the calculation of quark distribution functions here we take the dynamical quark mass in Eq. (3.1) to be constant and simulate the ultraviolet cutoff implied by the instanton vacuum by applying an external ultraviolet regularization to divergent quark loops. We shall show in detail that this is a legitimate approximation for the quantities considered here.

The effective action allows to compute hadronic correlation functions at low energies in the large-N_c limit. In particular, the nucleon in the effective theory at the large-N_c limit characterized by a classical pion field which binds the quarks (chiral quark-soliton model) [26]. In the nucleon rest frame the classical pion field is of "hedgehog" form:

$$U_{\text{cl}}(\mathbf{x}) = \exp\left[i\frac{x^a \tau^a}{r}P(r)\right], \quad r = |\mathbf{x}|, \tag{3.3}$$

where $P(r)$ is called the profile function, with $P(0) = -\pi$ and $P(r) \to 0$ for $r \to \infty$. The quarks are described by single-particle wave functions, which are the solutions of the Dirac equation in the background pion field, Eq. (3.3):

$$H(U_{\text{cl}})|n\rangle = E_n|n\rangle, \tag{3.4}$$

where

$$H(U_{\text{cl}}) = -i\gamma^0\gamma^k\partial_k + M\gamma^0 U_{\text{cl}}^{\gamma_5} \tag{3.5}$$

is the single-particle Dirac Hamiltonian in the classical background pion field. The spectrum of $H(U_{\text{cl}})$ includes a discrete bound-state level, whose energy is denoted by E_{lev}, as well as the positive and negative Dirac continuum, polarized by the presence of the pion field. The soliton profile $P(r)$ is determined by minimizing the static energy of the pion field, which is given by the sum of the energy of the bound-state level and the aggregate energy of the negative Dirac continuum, the energy of the free Dirac continuum $(U=1)$ subtracted [26],

$$E_{\text{tot}}[U_{\text{cl}}] = N_c\left[\sum_{\substack{n \\ \text{occup}}} E_n - \sum_{\substack{n \\ \text{occup}}} E_n^{(0)}\right]$$

$$= N_c E_{\text{lev}} + N_c \sum_{\substack{n \\ \text{neg cont}}} (E_n - E_n^{(0)}), \tag{3.6}$$

and in the leading order of the $1/N_c$ expansion the nucleon mass is given simply by the value of the energy at the minimum:

$$M_N = E_{\text{tot}}[U_{\text{cl}}]. \tag{3.7}$$

The expression for the energy of the pion field, Eq. (3.6), contains a logarithmic ultraviolet divergence due to the contribution of the Dirac continuum and requires ultraviolet regularization (see below).

In higher order of the $1/N_c$ expansion one must take into account the fluctuations of the pion field about its saddle-point value. A special role is played by the zero modes of the pion field. The minimum of the energy, Eq. (3.6c), is degenerate with respect to translations of the soliton field in space, and to rotations in ordinary and isospin space [for the hedgehog field, Eq. (3.3), the two types of rotations are equivalent]. Quantizing these zero modes gives rise to nucleon states with definite momentum and spin-isospin quantum numbers [26,54]. This is done by subjecting the hedgehog field, Eq. (3.3), to time-dependent translations and flavor rotations:

$$U_{\text{cl}}(\mathbf{x}) \to R(t)U_{\text{cl}}(\mathbf{x} - \mathbf{X}(t))R^{\dagger}(t), \tag{3.8}$$

where $R(t)$ is an SU(2) rotation matrix, and computing the functional integral over the collective coordinates within the $1/N_c$ expansion. The functional integral over translations, $\mathbf{X}(t)$, can be reduced to a Hamiltonian system describing the free motion of the soliton center of mass, with mass M_N, Eq. (3.7), whose eigenfunctions are plane waves with given three-momentum, $\exp(i\mathbf{P}\cdot\mathbf{X})$. [The $O(1/N_c)$ contribution of the collective translations to the nucleon mass can be ne-

glected in the applications considered here.] In the functional integral over collective rotations, $R(t)$, the rotational energy is given by

$$E_{\text{rotating soliton}} - E_{\text{static soliton}} = I \, \text{tr}[\Omega(t)\Omega(t)] + \cdots, \tag{3.9}$$

where

$$\Omega(t) \equiv \Omega_a(t)\frac{\tau^a}{2} = -iR^\dagger(t)\dot{R}(t) \tag{3.10}$$

is the angular velocity, and I is the moment of inertia of the soliton, which is given by a double sum over quark single-particle levels in the background pion field:

$$I = \frac{N_c}{6} \sum_{\substack{n \\ \text{occup}}} \sum_{\substack{m \\ \text{nonoccup}}} \frac{\langle n|\tau^a|m\rangle\langle m|\tau^a|n\rangle}{E_m - E_n}. \tag{3.11}$$

Here the sum over n runs over all occupied states, i.e., the discrete level and the negative Dirac continuum, the sum over m over all nonoccupied states, i.e., the positive Dirac continuum. (The ultraviolet regularization of this quantity will be discussed below.) It is important that the moment of inertia is of order N_c, so the typical angular velocities are

$$\Omega(t) \sim \frac{1}{N_c} \tag{3.12}$$

and one can compute the functional integral by expanding in powers of the angular velocity. To leading order in $1/N_c$ the collective motion is described by a Hamiltonian

$$H_{\text{rot}} = \frac{S_a^2}{2I} = \frac{T_a^2}{2I}, \tag{3.13}$$

where S_a and T_a are the right and left angular momenta, and the Hamiltonian, Eq. (3.13), has been obtained by the "quantization rule"

$$\Omega_a \rightarrow \frac{S_a}{I}. \tag{3.14}$$

This Hamiltonian describes a spherical top in spin-isospin space, subject to the constraint $S^2 = T^2$, which is a consequence of the "hedgehog" symmetry of the static pion field, Eq. (3.3). Its eigenfunctions, classified by $S^2 = T^2$, S_3, and T_3 are given by the Wigner finite-rotation matrices [26]:

$$\phi_{S_3 T_3}^{S=T}(R) = \sqrt{2S+1}(-1)^{T+T_3} D_{-T_3, S_3}^{S=T}(R). \tag{3.15}$$

The four nucleon states have $S = T = 1/2$, with $S_3, T_3 = \pm 1/2$, while for $S = T = 3/2$ one obtains the 16 states of the Δ resonance. The rotational energy $S(S+1)/(2I)$ gives a $1/N_c$ correction to the nucleon mass, which should be added to Eq. (3.7). In particular, the nucleon-Δ mass splitting is given by

$$M_\Delta - M_N = \frac{3}{2I}. \tag{3.16}$$

The saddle-point solution, Eq. (3.3), and the collective quantization procedure outlined above, not only give rise to nucleon states of definite momentum and spin-isospin quantum numbers in the effective chiral theory defined by Eq. (3.1); they also imply a prescription for the calculation of matrix elements of arbitrary composite quark operators between nucleon states. For a review of the applications of this model to baryon observables such as masses, form factors, etc., we refer to Ref. [36]. We shall apply this approach to calculate the nucleon's transversity distributions in Sec. III C.

B. Transversity distributions in the large-N_c limit

Before embarking on the calculation of the transversity distributions in the chiral quark soliton model it is useful to establish the large-N_c behavior of these distributions on general grounds [24,34]. Standard N_c counting tells us that at large N_c the tensor charges of the nucleon scale as

$$\delta u - \delta d \sim N_c, \quad \delta u + \delta d \sim 1; \tag{3.17}$$

i.e., the isovector matrix element is leading relative to the isosinglet one. This behavior is analogous to that of the axial charges, which scale as

$$g_A^{(3)} = \Delta u - \Delta d \sim N_c, \quad g_A^{(0)} = \Delta u + \Delta d \sim 1. \tag{3.18}$$

Combining Eq. (3.17) with the fact that in the large-N_c limit the parton distributions are concentrated at values of x of the order of $1/N_c$ one obtains that the transversity distributions at large N_c scale as

$$\delta u(x) - \delta d(x), \quad \delta\bar{u}(x) - \delta\bar{d}(x) \sim N_c^2 f(N_c x), \tag{3.19}$$

$$\delta u(x) + \delta d(x), \quad \delta\bar{u}(x) + \delta\bar{d}(x) \sim N_c f(N_c x), \tag{3.20}$$

where $f(y)$ is a stable function in the large-N_c limit, which depends on the particular distribution considered.

C. Calculation of the transversity distributions

We now outline the calculation of the transversity quark and antiquark distributions in the chiral quark soliton model. The methods for computing parton distributions at a low normalization point in this approach have been developed in Refs. [24,25,29], and we refer to these papers for all general methodological questions.

When computing quark-antiquark distribution in the effective chiral theory it is assumed that the normalization point of the distributions is of the order of the ultraviolet cutoff of the effective theory, i.e., of $\mathcal{O}(600 \text{ MeV})$. At this scale the QCD twist-2 quark operators can be identified with the corresponding operators in the effective theory. The gluon distributions are zero at this level of approximation [24]. A more explicit justification for this procedure is provided by the instanton picture of the QCD vacuum, which allows one to derive the low-energy effective theory. It was shown that in leading order of the packing fraction of the instanton medium the quark and antiquark distributions saturate the nucleon momentum and spin sum rule, while the

gluon distributions are zero [24,55]. The calculations of parton distributions in Refs. [24,25,29,38,39,56] were performed at this level of approximation. In the case of the transversity distributions, since there is no transversity gluon distribution, one may expect this "quark-antiquark-only" approximation to give even better results than in the unpolarized and longitudinally polarized case.

Having expressed the QCD operators in Eqs. (2.4),(2.5) in terms of the quark fields of the effective theory, we can now compute their nucleon matrix elements within the $1/N_c$ expansion, using standard techniques. It is convenient to work in the nucleon rest frame, where the classical pion field describing the nucleon (up to collective translations and rotations) is given by Eq. (3.3); in this frame the matrix elements defining the transversity distributions take the form of Eqs. (2.4),(2.5). Matrix elements of quark bilinear operators such as Eqs. (2.4),(2.5) can be reduced to those of time-ordered products of quark fields, which can be calculated with the help of the Feynman Green function of the quarks in the background pion field:

$$G_F(y^0,\mathbf{y};x^0,\mathbf{x}) = \langle y^0,\mathbf{y}|[i\partial_t - H(U)]^{-1}|x^0,\mathbf{x}\rangle. \quad (3.21)$$

Here the saddle-point pion field is the slowly rotating hedgehog field, Eq. (3.8). For this ansatz the Green function, Eq. (3.21), takes the form

$$[i\partial_t - H(U)]^{-1} = R(t)[i\partial_t - H(U_{\rm cl}) - \Omega(t)]^{-1} R^\dagger(t), \quad (3.22)$$

where $\Omega(t)$ is the angular velocity, Eq. (3.10). Performing the functional integral over collective coordinates of the saddle-point field as described in Sec. III A, projecting on nucleon states with definite momentum and spin-isospin quantum numbers one obtains the following "master formula" for the expectation value of a color-singlet time-ordered quark bilinear operator in the nucleon:

$$\langle \mathbf{P}=0,S=T,S_3,T_3|T\{\psi^\dagger(x)\Gamma\psi(y)\}|\mathbf{P}=0,S=T,S_3,T_3\rangle$$

$$= 2M_N \int d^3\mathbf{X} \int dR_1 \int dR_2 [\phi^{T=S}_{T_3S_3}(R_2)]^* \phi^{T=S}_{T_3S_3}(R_1)$$

$$\times \int^{R(T)=R_2}_{R(-T)=R_1} DR\, \mathrm{Det}[i\partial_t - H(U_{\rm cl}) - \Omega(t)]$$

$$\times (-i)N_c\, \mathrm{Tr}\!\left[R^\dagger(x^0)\Gamma R(y^0)\right.$$

$$\left.\times \left\langle y^0,\mathbf{y}-\mathbf{X}\left|\frac{1}{i\partial_t - H(U_{\rm cl})-\Omega(t)}\right|x^0,\mathbf{x}-\mathbf{X}\right\rangle\right]. \quad (3.23)$$

Here Γ denotes a matrix in Dirac spinor and isospin space, and $\mathrm{Tr}\cdots$ implies the trace over Dirac and flavor indices (the sum over color indices has already been performed).

The functional integral over rotations, $R(t)$, in Eq. (3.23) can be computed by expanding the integrand in the angular

velocity, Ω, Eq. (3.10), which is of order $1/N_c$. The expansion of the determinant of the Dirac operator gives rise to the "kinetic term"

$$\mathrm{Det}[i\partial_t - H(U_{\rm cl}) - \Omega(t)] \propto \exp\!\left[\frac{iI}{2}\int dt\, \Omega_a^2(t) + \cdots\right], \quad (3.24)$$

where I is the moment of inertia of the soliton, Eq. (3.11). The functional integral with this action can now be computed exactly; it corresponds to a rigid rotator described by the Hamiltonian, Eq. (3.13). In addition, one has to expand the quark Green function in Eq. (3.23) in powers of Ω. The minimum power of Ω required to obtain a nonzero result determines the order of the matrix element in the $1/N_c$ expansion, which is in general different for the different isospin components of the matrix element of a given operator.

Isovector transversity distribution. We now apply the above prescription to the calculation of the transversity distributions, Eqs. (2.4),(2.5). It turns out that in the case of the isovector transversity distribution the RHS of Eq. (3.23) is nonzero already in zeroth order of the expansion of the quark propagator in $\Omega(t)$, in agreement with the fact that this isospin component is leading in the $1/N_c$ expansion. The functional integral over rotations in leading order of $1/N_c$ (i.e., neglecting all time dependence of the collective rotation) just produces a delta function which enforces $R_1 = R_2$. The result can be written in the form

$$\delta u(x) - \delta d(x) = -(2S_3)2M_N \int d^3\mathbf{X} \int dR\, \phi^*_{T_3S_3}(R)O^{I=1}$$

$$\times (\mathbf{X},R;x)\phi_{T_3S_3}(R), \quad (3.25)$$

where $O^{I=1}$ is an operator in the space of functions of the collective coordinates:

$$O^{I=1}(\mathbf{X},R;x)$$

$$= (-i)N_c \int \frac{dz^0}{2\pi} e^{ixM_Nz^0}\, \mathrm{Tr}\!\left[R^\dagger\tau^3 R\frac{1+\gamma^0\gamma^1}{2}\gamma_5\gamma^3\right.$$

$$\left.\times\left\langle z^0,\mathbf{z}-\mathbf{X}\left|\frac{1}{i\partial_t-H(U_{\rm cl})}\right|0,-\mathbf{X}\right\rangle\right]_{z^1=-z^0,z_\perp=0}. \quad (3.26)$$

The integral over rotations is readily performed; one introduces the rotation matrix in the adjoint representation,

$$R^\dagger\tau^3 R = D_{3a}(R)\tau^a, \quad D_{ba}(R) \equiv \frac{1}{2}\mathrm{Tr}(\tau_b R\tau_a R^\dagger), \quad (3.27)$$

and makes use of the identity

$$\int dR\, \phi^*_{S_3T_3}(R)D_{3a}(R)\phi_{S_3T_3}(R) = -\frac{1}{3}(2T_3)(2S_3)\delta_{a3}. \quad (3.28)$$

For further evaluation one writes the quark Green function in the static classical pion field in Eq. (3.26) in frequency representation:

$$\left\langle z^0, \mathbf{z} - \mathbf{X} \left| \frac{1}{i\partial_t - H(U_{cl})} \right| 0, -\mathbf{X} \right\rangle$$

$$= \int \frac{d\omega}{2\pi} e^{-i\omega z^0} \left\langle \mathbf{z} - \mathbf{X} \left| \frac{1}{\omega - H(U_{cl})} \right| -\mathbf{X} \right\rangle$$

(3.29)

(the choice of contour for the ω integral will be discussed below), and brings the matrix element into diagonal form by introducing the finite-translation operator

$$\langle \mathbf{z} - \mathbf{X} | \cdots | -\mathbf{X} \rangle = \langle -\mathbf{X} | \exp(iP^k z^k) \cdots | -\mathbf{X} \rangle, \quad (3.30)$$

where P^k denotes the momentum operator in the space of quark single-particle wave functions, Eq. (3.4). In this way one obtains

$$\delta u(x) - \delta d(x)$$

$$= (2T_3) \frac{2M_N N_c}{3} (-i) \int \frac{d\omega}{2\pi}$$

$$\times \int d^3\mathbf{X} \, \mathrm{Tr} \left[\tau^3 \frac{1 + \gamma^0 \gamma^1}{2} \gamma_5 \gamma^3 \right.$$

$$\left. \times \left\langle -\mathbf{X} \left| \delta(xM_N - \omega - P^1) \frac{1}{\omega - H(U_{cl})} \right| -\mathbf{X} \right\rangle \right].$$

(3.31)

The delta function here is the result of integrating the exponential factors in Eqs. (3.26), (3.29), and (3.30) over z^0, keeping in mind the constraint $z^1 = -z^0$. In fact, the RHS of Eq. (3.31) has the form of a functional trace of an operator in the space of quark single-particle states, and can be written more concisely as (Sp denotes the functional trace)

$$\delta u(x) - \delta d(x) = (2T_3) \frac{2M_N N_c}{3} (-i) \int \frac{d\omega}{2\pi}$$

$$\times \mathrm{Sp} \left[\tau^3 \frac{1 + \gamma^0 \gamma^1}{2} \gamma_5 \gamma^3 \right.$$

$$\left. \times \delta(xM_N - \omega - P^1) \frac{1}{\omega - H(U_{cl})} \right].$$

(3.32)

In the above expressions vacuum subtraction is implied; i.e., one should subtract the corresponding expressions in which the Hamiltonian in the hedgehog pion field, Eq. (3.3), is replaced by the free Hamiltonian ($U=1$).

Equations (3.31) and (3.32) serve as the basis for the actual computation of the isovector distribution. An explicit expression, suitable for numerical calculations, can be derived by substituting in Eq. (3.32) the spectral representation of the quark Green function in the background pion field:

$$\frac{1}{\omega - H(U_{cl})} = \sum_{n \atop \text{occup}} \frac{|n\rangle\langle n|}{\omega - E_n - i0} + \sum_{n \atop \text{nonoccup}} \frac{|n\langle n|}{\omega - E_n + i0}.$$

(3.33)

Here, E_n and $|n\rangle$ are the single-particle eigenvalues and eigenstates of Eq. (3.4). The poles are shifted to the upper and lower halves of the ω plane, corresponding to whether the single-particle levels are occupied or not. Substituting Eq. (3.33) into Eq. (3.32) we obtain a representation of the isovector distribution as a sum over quark single-particle levels in the background pion field:

$$\delta u(x) - \delta d(x)$$

$$= (2T_3) \frac{N_c M_N}{3} \left(\sum_{n \atop \text{occup}} - \sum_{n \atop \text{nonoccup}} \right)$$

$$\times \langle n | \tau^3 \frac{1 + \gamma^0 \gamma^1}{2} \gamma_5 \gamma^3 \delta(xM_N - E_n - P^1) | n \rangle.$$

(3.34)

For many purposes it is desirable to have representations of the distribution function involving sums over only occupied, or only nonoccupied, levels. Such representations can be obtained from Eq. (3.34) if one notes that the sum over *all* levels of the matrix element on the RHS of Eq. (3.34) is zero:

$$\sum_{n \text{ all}} \left\langle n \left| \tau^3 \frac{1 + \gamma^0 \gamma^1}{2} \gamma_5 \gamma^3 \delta(xM_N - E_n - P^1) \right| n \right\rangle = 0.$$

(3.35)

This condition is actually equivalent to the locality condition of the anticommutator of quark fields in the effective low-energy theory, which ensures that one gets the same result for the distribution function in the chiral quark-soliton model if one starts from the QCD definition as the matrix element of the quark bilinear $\bar{\psi}(0) \cdots \psi(z)$, Eq. (2.1), or from the equivalent definition where as the matrix element of the QCD operator where $\bar{\psi}$ and ψ have been anticommuted, $-\psi(z) \cdots \bar{\psi}(0)$ [24,25]. It is crucial that the ultraviolet regularization of the effective low-energy theory does not destroy the property, Eq. (3.35), as has been discussed extensively in the context of the isoscalar unpolarized and isovector polarized distributions in Refs. [24,25]. A detailed investigation of the conditions under which Eq. (3.35) holds in the case of the isovector transversity distribution is presented in Sec. III E and the Appendix; here we shall simply take this property for granted. In particular, Eq. (3.35) can be read as saying that

$$\sum_{n \atop \text{occup}} \langle n | \cdots | n \rangle = - \sum_{n \atop \text{nonoccup}} \langle n | \cdots | n \rangle. \quad (3.36)$$

This allows to write, instead of Eq. (3.34),

$$\delta u(x) - \delta d(x) = (2T_3)\frac{2N_c M_N}{3} \sum_{\substack{n \\ \text{occup}}} \left\langle n \left| \tau^3 \frac{1+\gamma^0\gamma^1}{2} \gamma_5 \gamma^3 \right. \right.$$

$$\times \delta(xM_N - E_n - P^1) \left| n \right\rangle \quad (3.37)$$

$$= -(2T_3)\frac{2N_c M_N}{3} \sum_{\substack{n \\ \text{nonoccup}}} \left\langle n \left| \tau^3 \frac{1+\gamma^0\gamma^1}{2} \right. \right.$$

$$\times \gamma_5 \gamma^3 \delta(xM_N - E_n - P^1) \left| n \right\rangle. \quad (3.38)$$

All three representations of the isovector transversity distribution, Eqs. (3.34), (3.37), and (3.38), are equivalent provided Eq. (3.35) holds. In all cases, the corresponding expressions for the antiquark distributions are obtained from those for the quark distributions by the substitution, Eq. (2.5). It is understood that one should subtract from Eqs. (3.34), (3.37), and (3.38) the corresponding sums over eigenstates of the free Hamiltonian ($U=1$).

The expressions (3.37) and (3.38) can be used for numerical evaluation of the isovector distribution function; see Sec. IV B. In particular, we shall verify the equivalence of the two representations in the numerical calculations.

Isosinglet transversity distribution. The calculation of the isosinglet transversity distribution is slightly more complicated than that of the isovector one. In the isosinglet case a nonzero result is obtained only after expanding the integrand in Eq. (3.23) to first order in the angular velocity Ω. As a consequence this distribution is suppressed by a factor $1/N_c$ relative to the isosinglet one, in agreement with the general N_c-counting arguments of Sec. III B.

Quark distribution functions are given by matrix elements of nonlocal operators (quark bilinears at different space-time points). The Ω expansion of matrix elements of such operators poses some special problems, which have been discussed extensively in Ref. [29] in connection with the calculation of the isovector unpolarized distribution. Terms of first order in $\Omega(t)$ arise from the first-order expansion of the Green function in Eq. (3.23), as well as from expansion of the structure

$$R^\dagger(x^0)\Gamma R(y^0),$$

which is nonlocal in time.[2] There are thus two types of contributions to the distribution functions. For the isosinglet transversity distribution the result obtained after expanding to first order in Ω can be written as [cf. Eq. (3.25)]

---

[2] If one computed not the distribution function directly but its moments, the second type of contribution would arise from the presence of derivatives acting on the quark fields in the local twist-2 operators, which in the chiral quark-soliton model become time derivatives acting on the rotational matrices in Eq. (3.23).

$$\delta u(x) + \delta d(x) = -(2S_3)2M_N \int d^3\mathbf{X} \int dR \, \phi^*_{T_3 S_3}(R)$$

$$\times [O^{I=0,(1)} + O^{I=0,(2)}](\mathbf{X},R,S;x)\phi_{T_3 S_3}(R), \quad (3.39)$$

where

$$O^{I=0,(1)}(\mathbf{X},R,S;x)$$

$$= (-i)N_c \int \frac{dz^0}{2\pi} e^{ixM_N z^0} \text{Tr}\left[R^\dagger R \frac{1+\gamma^0\gamma^1}{2}\gamma_5\gamma^3 \right.$$

$$\times \left\langle z^0, \mathbf{z}-\mathbf{X} \left| \frac{1}{i\partial_t - H(U_{\text{cl}})} \left(\frac{i}{2I}S^a\tau^a \right) \right. \right.$$

$$\times \left. \frac{1}{i\partial_t - H(U_{\text{cl}})} \left| 0, -\mathbf{X} \right\rangle \right]_{z^1=-z^0, z_\perp=0}, \quad (3.40)$$

$$O^{I=0,(2)}(\mathbf{X},R,S;x)$$

$$= (-i)N_c \int \frac{dz^0}{2\pi} e^{ixM_N z^0} z^0 \, \text{Tr}\left[R^\dagger R \left(\frac{i}{2I}S^a\tau^a \right) \right.$$

$$\times \frac{1+\gamma^0\gamma^1}{2}\gamma_5\gamma^3 \left\langle z^0, \mathbf{z}-\mathbf{X} \right|$$

$$\times \left. \frac{1}{i\partial_t - H(U_{\text{cl}})} \left| 0, -\mathbf{X} \right\rangle \right]_{z^1=-z^0, \ z_\perp=0}. \quad (3.41)$$

Now the operators acting on the wave functions in collective coordinates involve also the spin operator S, which arises from replacing the angular velocity according to the "quantization rule," Eq. (3.14).

Note that in Eqs. (3.40) and (3.41) the spin operators do not commute with the rotational matrices, so in principle one should be careful about their ordering. However, it turns out that in the case of interest here there is no ordering ambiguity. By explicit calculation, using the methods described in Ref. [29], one can show that the commutator terms corresponding to the differences between different operator orderings give zero contribution in the final result.[3]

The integrals over rotational matrices in Eqs. (3.40) and (3.41) are nothing but the average of the spin operator in the rotational state:

---

[3] The absence of ordering ambiguities can be shown to be a general feature when computing $1/N_c$-suppressed quantities, such as the isosinglet transversity distribution considered here, in *leading nonvanishing order*, that is, at level Ω^1. Ordering ambiguities may arise, however, when considering $1/N_c$ corrections to quantities which are nonzero already in leading order of the $1/N_c$ expansion, e.g., in Ω^1 contributions to the isovector transversity distribution or to the isovector longitudinally polarized distribution. These difficulties cause a violation of the partially conserved axial vector current (PCAC) relation and are the subject of ongoing investigations.

$$\int dR \, \phi^*_{S_3 T_3}(R) S^a \phi_{S_3 T_3}(R) = S_3 \delta_{a3}. \qquad (3.42)$$

The further evaluation of the expressions proceeds largely in analogy to the isovector case. Passing to the frequency representation of the quark Green functions [cf. Eq. (3.29)] and making use of Eq. (3.30), the contributions, Eqs. (3.40) and (3.41), become

$$[\delta u(x) + \delta d(x)]^{(1)}$$

$$= \frac{N_c M_N}{4I} \int \frac{d\omega}{2\pi} \mathrm{Sp}\left[\frac{1 + \gamma^0 \gamma^1}{2} \gamma_5 \gamma^3 \delta(x M_N - \omega - P^1) \right.$$

$$\left. \times \frac{1}{\omega - H(U_{\mathrm{cl}})} \tau^3 \frac{1}{\omega - H(U_{\mathrm{cl}})} \right], \qquad (3.43)$$

$$[\delta u(x) + \delta d(x)]^{(2)}$$

$$= \frac{N_c}{4I}(-i) \frac{\partial}{\partial x} \int \frac{d\omega}{2\pi} \mathrm{Sp}\left[\tau^3 \frac{1 + \gamma^0 \gamma^1}{2} \gamma_5 \gamma^3 \right.$$

$$\left. \times \delta(x M_N - \omega - P^1) \frac{1}{\omega - H(U_{\mathrm{cl}})} \right]. \qquad (3.44)$$

The derivative in x in Eq. (3.44) results from the factor of z^0 present in Eq. (3.41). One notes that this contribution is, up to a factor, equal to the derivative in x of the leading-order $\mathcal{O}(\Omega^0)$ result for the isovector transversity distribution, Eq. (3.32):

$$[\delta u(x) + \delta d(x)]^{(2)} = -\frac{3}{2IM_N} \frac{\partial}{\partial x}[\delta u(x) - \delta d(x)]^{\mathrm{leading}}. \qquad (3.45)$$

Substituting here Eqs. (3.37) or (3.38) one obtains a representation of this contribution as a simple sum over (occupied or nonoccupied) quark single-particle levels. For the contribution (1), Eq. (3.43), a representation as a double sum over quark levels can be derived, following the steps outlined in Appendix A of Ref. [29]. Again one substitutes the spectral representations, Eq. (3.33), for the two quark propagators. A subtle point is the occurrence of a double pole in the ω integral for those terms where the energies in the two denominators coincide; see Ref. [29] for details. Assuming a quasidiscrete spectrum of levels, as appropriate for numerical calculations using a finite box, and separating explicitly the contributions of levels with $E_m \neq E_n$ and $E_m = E_n$ in the double sum over levels n and m one obtains a representation of the isosinglet transversity distribution in the form

$$[\delta u(x) + \delta d(x)]^{(1)}$$

$$= \frac{N_c M_N}{4I} \left(\sum_{\substack{n \\ \mathrm{occup}}} - \sum_{\substack{n \\ \mathrm{nonoccup}}} \right) \left\{ 2 \sum_{\substack{m \\ E_m \neq E_n}} \frac{1}{E_m - E_n} \langle n|\tau^3|m\rangle \right.$$

$$\times \left\langle m \left| \frac{1 + \gamma^0 \gamma^1}{2} \gamma_5 \gamma^3 \delta(E_n + P^1 - x M_N) \right| n \right\rangle$$

$$- \sum_{\substack{m \\ E_m = E_n}} \langle n|\tau^3|m\rangle \left\langle m \left| \frac{1 + \gamma^0 \gamma^1}{2} \gamma_5 \gamma^3 \right. \right.$$

$$\left. \left. \times \delta'(E_n + P^3 - x M_N) \right| n \right\rangle \right\}. \qquad (3.46)$$

As in the case of the isovector distribution, one can show that the sum over *all* levels n of the terms in braces in Eq. (3.46) is zero (see Sec. III E and the Appendix),

$$\sum_{\substack{n \\ \mathrm{all}}} \{\cdots\} = 0, \qquad (3.47)$$

so that we can write Eq. (3.46) equivalently as

$$[\delta u(x) + \delta d(x)]^{(1)} = \frac{N_c M_N}{2I} \sum_{\substack{n \\ \mathrm{occup}}} \{\cdots\} \qquad (3.48)$$

$$= -\frac{N_c M_N}{2I} \sum_{\substack{n \\ \mathrm{nonoccup}}} \{\cdots\}. \qquad (3.49)$$

Expressions (3.48) and (3.49), as well as Eq. (3.45) together with Eqs. (3.37) and (3.38), will be used in the numerical calculation of the isosinglet transversity distribution in Sec. IV B.

D. Ultraviolet regularization

The effective chiral theory used to describe the nucleon is nonrenormalizable and understood to be defined with an explicit ultraviolet cutoff. When calculating parton distributions in this approach one must ensure that none of their essential properties, such as positivity, sum rules, etc., are violated by the ultraviolet regularization. For the isoscalar-unpolarized and isovector-polarized distributions this problem has been studied in detail in Refs. [24,25]. These distributions were found to contain ultraviolet divergences which require regularization, and it was shown that a possible regularization, preserving all important properties of the parton distributions, is by way of a Pauli-Villars subtraction.

We now discuss the issue of ultraviolet regularization in the case of the transversity distributions. Our investigation consists of two parts. First, we show that the expressions for the transversity distributions in the effective low-energy theory are in fact ultraviolet finite, and thus can in principle be computed without an ultraviolet cutoff. Second, we investigate the role of ultraviolet regularization in the "locality" conditions, Eqs. (3.35) and (3.47), which ensure the equivalence of the representations of the transversity distributions as sums over occupied and nonoccupied quark levels. In Sec. III E we describe an interesting anomaly-type phenomenon found in these sums over quark levels, which takes the form of noncommutativity of the chiral limit and the limit of infinite ultraviolet cutoff.

In order to investigate the dependence of the transversity distributions calculated in the effective low-energy theory on

the ultraviolet cutoff, we consider the formal limit of large soliton size, in which one can derive explicit expressions for the distributions as functionals of the classical pion field, $U_{\rm cl}(\mathbf{x})$ (gradient expansion) [24,25]. The gradient expansion can immediately be derived from the representations of the distribution functions as functional traces with the quark Green function, Eq. (3.32) in the isovector case and Eqs. (3.43) and (3.44) in the isoscalar case, if one substitutes an approximate form of the quark Green function, appropriate for small gradients of the classical pion field, $\nabla_k U_{\rm cl}(\mathbf{x}) \ll M$ ($k=1,2,3$):

$$\frac{1}{\omega - H(U_{\rm cl})} = \frac{\omega + H(U_{\rm cl})}{\omega^2 - H^2(U_{\rm cl})}$$

$$= \frac{1}{\omega^2 + \nabla^2 - M^2 - iM(\slashed{\nabla} U_{\rm cl}^{\gamma_5})}$$

$$\times (\omega - i\gamma^0 \gamma^k \nabla_k + M\gamma^0 U_{\rm cl}^{\gamma_5})$$

$$= \frac{1}{\omega^2 + \nabla^2 - M^2} \sum_{n=0}^{\infty} \left[iM(\slashed{\nabla} U_{\rm cl}^{\gamma_5}) \frac{1}{\omega^2 + \nabla^2 - M^2} \right]^n$$

$$\times (\omega - i\gamma^0 \gamma^k \nabla_k + M\gamma^0 U_{\rm cl}^{\gamma_5}). \qquad (3.50)$$

In this formal expansion increasing numbers of gradients of $U_{\rm cl}(\mathbf{x})$ come with increasing inverse powers of ω and momentum, so that the leading ultraviolet divergences (if any) of the distributions can be read off from the leading-order gradient expansion.

Isovector transversity distribution. In the case of the isovector transversity distribution the first nonvanishing contribution in Eq. (3.32) comes from the term with $n=2$ in the expansion, Eq. (3.50). Computing the resulting functional trace using a basis of plane-wave states one obtains the leading-order gradient expansion in the form

$$[\delta u(x) - \delta d(x)]^{\rm grad\,exp} = \int_{-\infty}^{\infty} d\xi \, e^{i\xi M_N x} f^{I=1}(\xi),$$

$$f^{I=1}(\xi) = \frac{N_c M_N M}{48\pi^3} \int_0^1 d\alpha \int_0^\alpha d\beta \int d^3z$$

$$\times \mathrm{tr}_{\rm fl} \{ U_{\rm cl}(\mathbf{z} - \alpha\xi\mathbf{e}_3)$$

$$\times [\partial_i U_{\rm cl}^\dagger(\mathbf{z} - \beta\xi\mathbf{e}_3)][\partial_j U_{\rm cl}(\mathbf{z})]\tau^k \}$$

$$\times [(\varepsilon^{i2j}\delta^{k1} + \varepsilon^{1ij}\delta^{k2})$$

$$+ i(\varepsilon^{1ij}\delta^{k1} - \varepsilon^{i2j}\delta^{k2})]. \qquad (3.51)$$

We note that in deriving this result we have assumed that the classical pion field drops faster than $1/r^2$ for $r \to \infty$. This behavior is required in order to be able to drop certain surface terms involving the pion field at $r = \infty$, which arise from terms in Eq. (3.50) with $n=0$ and 1. Such contributions are

at the heart of the anomaly-type phenomenon described in Sec. III E and the Appendix, and we shall return to this point there.

The gradient expansion, Eq. (3.51), tells us that the isovector transversity distribution is ultraviolet finite: the ω integral in Eq. (3.32) is convergent. Thus this distribution does not require the ultraviolet cutoff of the effective theory and can be computed in the limit of infinite cutoff. We further note that the gradient expansion result for the isovector distribution is real. By explicit calculation one can show that of $f^{I=1}(\xi)$, Eq. (3.51) the real part is even, the imaginary part odd in ξ.

Isosinglet transversity distribution. In a similar way one can derive the gradient expansion for the isosinglet transversity distribution. (We do not quote the expressions here.) The gradient expansion shows that this distribution is finite in the limit of large UV cutoff and does not require regularization.

E. Anomaly-type phenomenon in the tensor charge

The tensor charges and, more generally, the transversity distributions show an interesting anomaly-type phenomenon, which we shall discuss now. In addition to of being of general interest, this anomaly has direct implications for our procedure of calculating the transversity distributions in the chiral quark-soliton model, as it is related to the equivalence of the representations of the distributions as sums over occupied or nonoccupied quark levels, Eqs. (3.37) and (3.38). This is equivalent to the condition that the sum of the single-particle matrix elements over all levels (i.e., occupied and nonoccupied) be zero, Eq. (3.35). A thorough understanding of this phenomenon is thus necessary for a reliable calculation of the distributions. In this section we illustrate the essential points by considering the simplest case of the isovector tensor charge; the corresponding calculation for the x-dependent distribution function presents only technical difficulties and is presented in the Appendix.

Anomaly in the tensor charge. At its most general, the anomaly we are dealing with is a statement about the functional trace of a chirally odd operator in the space of quark single-particle wave functions in a chiral background field. Let us consider the following functional trace:

$$\mathrm{Sp}[\tau^a \gamma_0 i\sigma_{0k}\gamma_5], \qquad (3.52)$$

which appears in the expression for the tensor charge. Naively this trace would be zero because the corresponding matrix traces in flavor and spin spaces are zero. However, actually we deal here with an uncertainty of the type $0 \cdot \infty$. To resolve this uncertainty one has to introduce a regularization. We choose here for illustrative purposes to regularize the trace (3.52) in the following way:

$$\mathrm{Sp}[\tau^a \gamma_0 i\sigma_{0k}\gamma_5]_{\rm reg} = \lim_{\epsilon \to 0} \mathrm{Sp}[\tau^a \gamma_0 i\sigma_{0k}\gamma_5 e^{-\epsilon H^2}]. \qquad (3.53)$$

Here

$$H^2(U) = -\nabla^2 + M^2 + iM(\slashed{\nabla} U^{\gamma_5}) \qquad (3.54)$$

is the Hamiltonian squared of the chiral quark-soliton model. In the limit of small ϵ the expression on the RHS of Eq. (3.53) can be computed analytically with the help of a semiclassical expansion. The leading contribution has the following form:

$$\lim_{\epsilon \to 0} \mathrm{Sp}[\tau^a \gamma_0 i \sigma_{0k} \gamma_5 e^{-\epsilon H^2}] = \frac{iM}{2\pi\sqrt{\pi\epsilon}} \int d^3x \, \partial_k \, \mathrm{tr}[\tau^a U(\mathbf{x})].$$
$$(3.55)$$

We see that the trace (3.53) is linearly divergent provided the chiral field $U(\mathbf{x})$ falls off not too rapidly at spatial infinity. For the soliton solution in the chiral limit the chiral field behaves at the spatial infinity as $U(\mathbf{x}) - 1 \sim x^a \tau^a / |\mathbf{x}|^3$, which leads to a nonzero coefficient in front of the linear divergence $1/\sqrt{\epsilon}$. The corresponding coefficient can be computed in terms of axial charge of the nucleon g_A keeping in mind the asymptotics of the soliton solution in the chiral limit:

$$U(\mathbf{x}) \sim 1 - i \frac{3g_A}{8\pi F_\pi^2} \frac{x^a \tau^a}{|\mathbf{x}|^3}.$$
$$(3.56)$$

The result has the form

$$\lim_{\epsilon \to 0} \mathrm{Sp}[\tau^a \gamma_0 i \sigma_{0k} \gamma_5 e^{-\epsilon H^2}] = \frac{g_A M}{2\pi F_\pi^2 \sqrt{\pi\epsilon}} \delta_k^a. \quad (3.57)$$

Note, however, that in the case of nonzero quark masses (however small they are) the linear divergence and hence the anomaly are zero. For calculations in a finite volume the condition for the absence of the anomaly is $M_\pi \times$ box size $\gg 1$. When computing the tensor charge (or the transversity distribution) by summing over quark levels in a finite volume, in the strict chiral limit one would find that the summation over occupied levels, Eq. (3.37), and nonoccupied levels, Eq. (3.38), does not give equivalent results; rather, the difference diverges linearly with the ultraviolet cutoff. This is indeed what we observe in the numerical calculations.

Elimination of the anomaly in the numerical calculations. In the numerical calculations, which are based on diagonalization of the Dirac Hamiltonian in a finite box, it is important to eliminate the "anomaly," Eq. (3.57). A way to do this is to modify the soliton profile at large distances in a way that it vanishes faster than $1/r^2$. For example, one may use a modified version of the variational profile suggested in Ref. [26],

$$P_{M_\pi}(r) = -2 \arctan\left[\frac{r_0^2}{r^2}(1 + M_\pi r)\exp(-M_\pi r)\right],$$
$$(3.58)$$

where $r_0 \approx 1.0 M^{-1}$ is the usual soliton size parameter. For $M_\pi \neq 0$ this profile decays exponentially at large r, while for small r it differs only very little from the massless profile. The "anomaly," Eq. (3.57), can then be made arbitrarily small by choosing the radius of the box used in the numerical calculation, D, sufficiently large so that

$$M_\pi D \gg 1. \tag{3.59}$$

The limit $M_\pi \to 0$ is then taken at the very end of the calculation by extrapolation of the numerical data. A measure of the successful elimination of the "anomaly" in the numerical calculations is the equivalence of the results obtained summing over occupied and nonoccupied states. In the actual calculations we have used values of M_π of the order of $(0.3–0.6)M$ and a box radius of 20 M^{-1}. For these parameters we observed equivalence of summing over occupied and nonoccupied states at the level of $(1–2)\%$.

IV. RESULTS

A. Transversity vs longitudinally polarized distributions

Having derived the expressions for the transversity distributions in the effective low-energy theory, we now proceed to compute the distributions and discuss their properties. Before turning to the numerical evaluation of the expressions it is instructive to compare the expressions for the transversity quark and antiquark distributions with those of the corresponding longitudinally polarized distributions at a qualitative level. In Sec. IV B we shall then compare the numerical results.

Since the nucleon's axial and tensor charges are the same in the nonrelativistic quark model, it is generally thought that differences between the two distributions are a measure of "relativistic effects" in the nucleon. The chiral-quark soliton model, which is a fully relativistic description of the nucleon, offers the unique possibility to study "relativistic effects" in the quark and antiquark distributions in a controlled way. The relevant parameter here is the "soliton size," i.e., the radius of the classical pion field of the nucleon. Although in reality the soliton size is determined by the minimization of the classical energy, Eq. (3.6), it is instructive to regard it as a parameter and to study the dependence of quantities such as the quark and antiquark distribution functions on it [58]. For small soliton sizes the bound-state level of quarks becomes weakly bound, and the lower Dirac components in its wave function become small. It was shown that in this limit nucleon matrix elements of a variety of local operators tend to their corresponding values in the nonrelativistic quark model [58]. On the other hand, in the limit of large soliton sizes the bound-state level approaches the negative continuum, and one may perform an expansion of nucleon matrix elements in inverse soliton size, which technically is obtained by expanding in gradients of the classical pion field (gradient expansion). In this limit this picture of the nucleon shows many similarities with the Skyrme model. In this sense one may say that the chiral quark-soliton model interpolates between the nonrelativistic quark model and a Skyrme soliton picture of the nucleon.

The quark model limit (small soliton size). It is thus interesting to study the transversity and longitudinally polarized distributions in dependence on the soliton size. Consider first the isovector distributions, which are leading in the $1/N_c$ expansion and both given by simple sums over quark single-particle levels; see Eq. (3.37) and Ref. [24]. For small soliton size the contributions due to the polarized Dirac continuum

become negligible, and both sums are dominated by the contribution from of the bound-state level:

$$
\left.\begin{array}{c}
[\delta u(x)-\delta d(x)]_{\text{lev}} \\
[\Delta u(x)-\Delta d(x)]_{\text{lev}}
\end{array}\right\}
$$

$$
=(2T_3)\frac{2N_c M_N}{3}\int\frac{d^3k}{(2\pi)^3}\Phi^{\dagger}_{\text{lev}}(\mathbf{k})
$$

$$
\times\left\{\begin{array}{c}
\tau^3\dfrac{1+\gamma^0\gamma^1}{2}\gamma_5\gamma^3\delta(xM_N-E_n-k^1) \\
(-)\tau^3\dfrac{1+\gamma^0\gamma^3}{2}\gamma_5\delta(xM_N-E_n-k^3)
\end{array}\right\}\Phi_{\text{lev}}(\mathbf{k}).
$$

$$(4.1)$$

Evaluating this contribution using the explicit form of the bound-state level wave function [26] one finds [24,34]

$$
[\delta u(x)-\delta d(x)]_{\text{lev}}
$$

$$
=\frac{N_c M_N}{3}\int_{|xM_N-E_{\text{lev}}|}^{\infty}\frac{dk}{2k}\left\{h(k)-j(k)\frac{xM_N-E_{\text{lev}}}{k}\right\}^2, \quad(4.2)
$$

$$
[\Delta u(x)-\Delta d(x)]_{\text{lev}}
$$

$$
=\frac{N_c M_N}{3}\int_{|xM_N-E_{\text{lev}}|}^{\infty}\frac{dk}{2k}\left\{h^2(k)+\left[2\frac{(xM_N-E_{\text{lev}})^2}{k^2}-1\right]\right.
$$

$$
\left.\times j^2(k)-2\frac{(xM_N-E_{\text{lev}})}{k}h(k)j(k)\right\}, \quad(4.3)
$$

where $h(k)$ and $j(k)$ are the Fourier transforms of the radial wave functions corresponding to the upper and lower components of the Dirac spinor wave function (see Appendix B of Ref. [24] for details). From the Dirac equation in the hedgehog pion field it follows that in the limit of small soliton size the lower Dirac component of the level wave function becomes small, $j(k)\rightarrow0$, so that the bound state effectively becomes nonrelativistic. One sees that in this case the expressions for the isovector transversity and longitudinally polarized distributions coincide.

In a similar way one may investigate the limit of small soliton size in the isoscalar polarized distributions. This is slightly more complicated, as these distributions are given by double sums over quark levels. Consider the representation of the isoscalar distribution in the form of a spectral integral, Eqs. (3.43) and (3.44). One can show that in the limit of small soliton size the dominant contribution is the sum of two contributions which one obtains by replacing one of the propagators in Eq. (3.43) by the pole associated with the bound-state level, $|\text{lev}\rangle\langle\text{lev}|/(\omega-E_{\text{lev}})$, the other one by the free propagator $1/(\omega-M)$. In this way one can show that also in the isoscalar case the transversity and longitudinally polarized contributions tend to the same function in the ''quark model'' limit.

The ''Skyrmion'' limit (large soliton size). In the formal limit of large soliton size the bound-state level of quarks

disappears in the negative-energy Dirac continuum. In this limit functions of the soliton field can be computed by expanding in gradients of the pion field, more precisely in the parameter $\partial U/M$. The techniques for deriving the gradient expansion of quark and antiquark distributions have been developed in Refs. [24,25]. For the isovector transversity distribution the result of the leading-order gradient expansion has been given in Eq. (3.51). The corresponding expression for the isovector longitudinally polarized distribution has been derived in Ref. [24],[4]

$$
\left.\begin{array}{c}
\Delta\bar{u}(x)-\Delta\bar{d}(x) \\
\Delta u(x)-\Delta d(x)
\end{array}\right\}\sim\frac{F_{\pi}^2 M_N}{3}\int_{-\infty}^{\infty}\frac{d\xi}{2\pi}\frac{\cos M_N\xi x}{\xi}\int d^3y
$$

$$
\times\text{tr}[\tau^3(-i)U_{\text{cl}}(\mathbf{y}+\xi\mathbf{e}_3)U^{\dagger}_{\text{cl}}(\mathbf{y})],
$$

$$(4.4)$$

where F_{π} is the pion decay constant:

$$
F_{\pi}^2=4N_c\int\frac{d^4k}{(2\pi)^4}\frac{M^2}{(M^2+k^2)^2}-\frac{M^2}{M_{PV}^2}4N_c
$$

$$
\times\int\frac{d^4k}{(2\pi)^4}\frac{M_{PV}^2}{(M_{PV}^2+k^2)^2}
$$

$$
=\frac{N_c M^2}{4\pi^2}\log\frac{M_{PV}^2}{M^2}. \quad(4.5)
$$

(In the last line we have given the result in the case when the logarithmic divergence of the integral is regularized by a Pauli-Villars subtraction.) Comparing the two expressions we see that in the limit of $r_0\rightarrow\infty$ (r_0 is the parameter characterizing the soliton size) the isovector transversity distribution, Eq. (3.51), is suppressed relative to the longitudinally polarized one, Eq. (4.4), by a factor of $1/(Mr_0)$. Thus we see that in this limit the two distributions behave differently at a qualitative level. This is not unexpected, since, as explained above, the limit of large soliton size can be regarded as the opposite of the nonrelativistic limit.

In the previous calculation of the isovector polarized quark distributions in the chiral quark-soliton model [24,25] it was observed that the gradient expansion expression, when evaluated at the the physical soliton size, gives a fairly realistic description of the isovector polarized *antiquark* distribution. (The *quark* distribution, in contrast, is poorly described by the gradient expansion expression.) The same can be expected to apply to the isovector transversity distribution. If this is so, it implies that we should expect the isovector transversity antiquark distribution to be smaller than the corresponding longitudinally polarized one, since the latter is

---

[4]The isovector longitudinally polarized quark and antiquark distributions coincide only in the hypothetical limit of large soliton size. For finite soliton sizes they are, of course, different.

parametrically suppressed in the soliton size. This expectation is indeed borne out by the numerical results, as will be shown in Sec. IV B.

The behavior of the isosinglet polarized distribution in the limit of large soliton size can also be studied using gradient expansion. The gradient expansion is readily derived from the spectral representation of the distribution functions, Eqs. (3.43) and (3.44), by formally expanding the quark propagators in powers of derivatives of the pion field, as discussed in Sec. III D; cf. Eq. (3.50). We shall not quote the lengthy expressions here. Rather, we shall discuss the properties of these distributions at the hands of the exact numerical results in Sec. IV B.

B. Numerical results

We now turn to the numerical evaluation of the transversity distributions in the chiral quark-soliton model. The numerical calculations are based on the expressions of the transversity quark and antiquark distributions as sums over quark levels in the classical pion field of the soliton, Eq. (3.34) for the isovector and Eq. (3.46) for the isosinglet distribution. In fact, in the actual calculations we prefer to use the representations of the distributions as sums over either occupied or nonoccupied levels, Eqs. (3.37) and (3.38), viz. Eqs. (3.48) and (3.49); a check of the equivalence of the summation over occupied or nonoccupied states offers a very powerful check of the numerical procedure.

Numerical method. The numerical method for evaluating the sums over single-particle quark levels has been described in Ref. [25]; see also Ref. [29]. The spectrum of quark levels is made quasidiscrete by placing the soliton in a spherical three-dimensional box, imposing so-called Kahana-Ripka boundary conditions [59]. The eigenvalues and eigenfunctions of the Dirac Hamiltonian in the background pion field are then found by numerical diagonalization, using the eigenstates of the free Hamiltonian (zero pion field) as a basis. One can then compute the sum over quark levels, using the fact that the matrix elements of the single-particle operators appearing in Eqs. (3.34) and (3.46) between the basis states are either known or can easily be computed numerically (see Ref. [25] for details).

Since the Hamiltonian is invariant under combined spin-isospin rotations and the basis states are eigenstates of the sum of the total angular momentum and isospin, it is advantageous to convert the expressions for the distribution functions, Eqs. (3.34) and (3.46), to a spherically symmetric form before performing the sums over levels. In this way one greatly reduces the number of nonzero matrix elements of the relevant single-particle operators between basis states. This symmetrization is achieved by replacing in Eqs. (3.34) and (3.46) the one- and three-vector components of the momentum operator, gamma matrices, and isospin matrices, by components along two orthogonal three-dimensional unit vectors **n** and **m**, and averaging over their orientations, with the constraint $\mathbf{n} \cdot \mathbf{m} = 0$. The matrix elements of the resulting "spherically symmetric" single-particle operators between basis states of angular momentum plus isospin can then easily be computed.

In the calculation of quark and antiquark distributions in the chiral quark-soliton model an additional complication arises due to the fact that the relevant single-particle operators are discontinuous functions of the single-particle momentum and energy operators, which leads to problems when performing the sums over of quark levels in a discrete basis. It was shown in Ref. [25] that this problem can easily be circumvented by applying Gaussian smearing in the variable x to expressions for the distribution functions. We shall apply this method here, using a smearing width of $\gamma = 0.1$; see Ref. [25] for details.

In the numerical calculations we have used the soliton profile determined in a self-consistent minimization of the soliton energy calculated with a Pauli-Villars cutoff [56]. In the case of the isosinglet unpolarized distribution this choice of profile, combined with a corresponding Pauli-Villars regularization of the distribution functions, allowed us to preserve the momentum sum rule for the flavor-singlet quark plus antiquark distributions. In the case of the transversity distributions, as shown in Sec. III D, the expressions for the distribution functions are ultraviolet finite, and there are no sum rules linking them to any quantity requiring regularization. For reasons of consistency in the choice of model parameters we compute also these distributions with the soliton profile, nucleon mass, and moment of inertia, calculated with the Pauli-Villars regularization of Ref. [56].

Although the transversity distributions are ultraviolet finite, numerical calculations require that we first evaluate the sums over levels, Eqs. (3.34) and (3.46), applying some smooth cutoff for levels with large energies, which at the end of the calculation is removed by extrapolation to infinity. When performing the numerical calculations in a finite-size box, it is important to take into account the "anomaly-type" phenomenon, described in detail in the Appendix. The nature of this phenomenon is noncommutativity between the limit of infinite energy cutoff and the chiral limit. In the strict chiral limit, where the soliton profile falls off like $P(r) \sim 1/r^2$ for $r \to \infty$, the sums over occupied and nonoccupied quark levels would no longer be equivalent. For this reason it is essential to perform the numerical calculations in the box with a soliton profile of finite range—for example, with a profile falling off as $\exp(-M_\pi r)/r$ for $r \to \infty$, where M_π is a parameter (not necessarily equal to the physical pion mass)—and extrapolate to $M_\pi \to 0$ at the end. The condition which must be satisfied for a proper calculation in a finite box is $M_\pi D \gg 1$, where D is the box radius (see the Appendix). If this condition is satisfied, one observes the equivalence of the results of the summation over occupied and nonoccupied states in the numerical calculations. In the actual calculations we have used a box size of $D = (20\text{–}30)M^{-1}$ and values of M_π in the range $(0.3\text{–}0.6)M$.

Numerical results. The numerical results for the isovector transversity distributions are shown in the upper plot of Fig. 1. It is interesting to first compare the relative contributions of the bound-state level (dashed line) and of the Dirac continuum (dotted line) of quarks to the quark and antiquark distributions. Figure 1 shows that the bound-state level gives the numerically dominant contribution to both the quark and antiquark transversity distributions. This is in agreement with
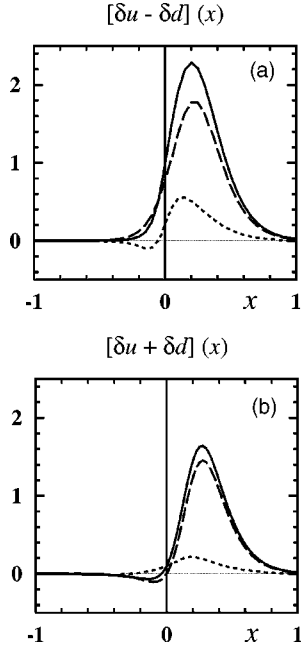
FIG. 1. The isovector (top) and isoscalar (bottom) transversity quark and antiquark distributions obtained from the chiral quark-soliton model. The functions shown here represent $[\delta u \mp \delta d](x)$ at $x>0$ and $-[\delta\bar{u} \mp \delta\bar{d}](-x)$ at $x<0$. Dashed lines: contributions of the bound-state level. Dotted lines: contributions of the Dirac continuum. Solid lines: total results (sums of bound-state level and Dirac continuum).

the observation that the isovector distribution is suppressed in gradient expansion, since the gradient expansion expression may be regarded as an estimate of the Dirac continuum contribution. Our results justify the approximation made by some of us in Ref. [34], where only the level contribution to the isovector transversity distributions was retained. Figure 2 (right column) shows the isovector quark and antiquark distributions multiplied by x. The antiquark distributions are shown separately in Fig. 3. Note that our approach predicts a definite sign for the isovector antiquark distribution, $\delta\bar{u}(x) - \delta\bar{d}(x)<0$. In the numerical calculation at the physical soliton radius this happens because of the dominance of the level contribution, which has a positive sign; see Fig. 1. The gradient expansion, Eq. (3.51), which becomes exact in the limit of large soliton size, also predicts a negative sign of $\delta\bar{u}(x) - \delta\bar{d}(x)$. As it is insensitive to the soliton size, the sign of the isovector antiquark distribution can be taken as a robust prediction of this model.

The different contributions to the isoscalar transversity distribution are shown in the lower plot of Fig. 1. One sees that in the isoscalar case the dominance of the level contribution is even more pronounced than in the isovector case. In particular, in the isoscalar antiquark distribution the level and continuum contributions all but cancel, leaving the total isoscalar antiquark distribution to be much smaller than the quark distribution (by a factor of the order of $1-2\times10^{-2}$, the precise value depending on x).

Comparing with the longitudinally polarized distributions. It is interesting to compare the numerical results for
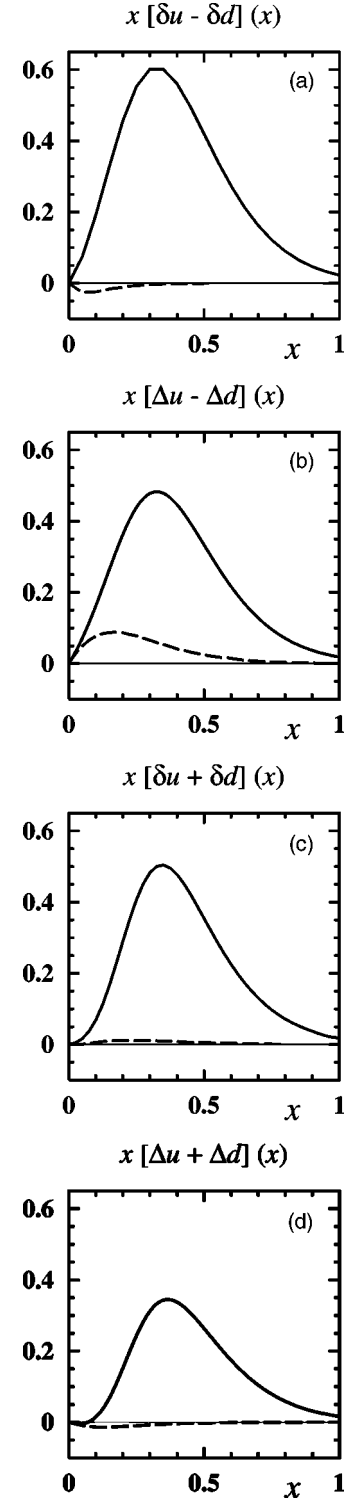

FIG. 2. The total isovector (a),(b) and isoscalar (c),(d) transversity and longitudinally polarized quark and antiquark distributions, multiplied by x. Shown are the total results (sum of level and continuum contributions), corresponding to the solid lines in Fig. 1. Solid lines: quark distributions. Dashed lines: antiquark distributions.

the transversity distributions with those of the longitudinally polarized distributions [38,39], which are shown in the right column of Fig. 2. One notices that, generally speaking, the
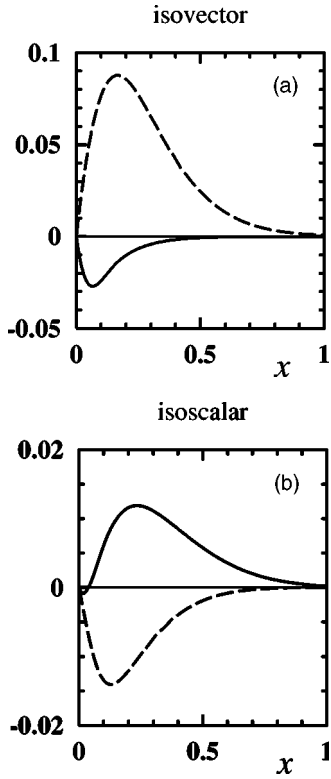
FIG. 3. The transversity and longitudinally polarized antiquark distributions; see Fig. 2. Top: isovector distributions $x[\delta\bar{u} - \delta\bar{d}](x)$ and $x[\Delta\bar{u} - \Delta\bar{d}](x)$. Bottom: isoscalar distributions $x[\delta\bar{u} + \delta\bar{d}](x)$ and $x[\Delta\bar{u} + \Delta\bar{d}](x)$. Solid lines: transversity antiquark distributions. Dashed lines: longitudinally polarized antiquark distributions.

quark distributions are of similar shape, although of different magnitude. The ratios of the numerical results for the transversity to the longitudinally polarized quark distributions are well described by the forms

$$\frac{\delta u(x) - \delta d(x)}{\Delta u(x) - \Delta d(x)} \approx 1.25, \tag{4.6}$$

$$\frac{\delta u(x) + \delta d(x)}{\Delta u(x) + \Delta d(x)} \approx 2.0 - 1.5x. \tag{4.7}$$

These fits apply for values of $x > 0.1$. (Note that our model, at the present level of approximation, cannot be applied to study the small-x behavior of the parton distributions at the low scale. Anyway, it is the intermediate- and large-x regions of the distributions at the low scale of the model which determine the behavior of the distributions in the small-x region at experimentally relevant scales due to perturbative evolution.) Note that this parametrization is a purely numerical fit. We find it useful to represent the results in this way, since we believe the ratios of distributions to be less model dependent than the distributions themselves. In our estimates of spin asymmetries in Sec. V we shall use these ratios, together with a parametrization of the longitudinally polarized distributions obtained from fits to inclusive DIS data.

Comparing the transversity and longitudinally polarized antiquark distributions we see that they are very different. This is in accordance with the fact that the two isovector distributions appear in different orders of the gradient expansion; see Sec. III D. It would thus not be useful to parametrize their ratio, the more since the standard parametrizations for the longitudinally polarized distributions exhibit large differences in the polarized antiquark distributions.[5] When computing observables one should rather use the results for these distributions directly.

Results for tensor charges. The tensor charges can be obtained by integrating the numerical results for the transversity distributions or directly by computing the matrix elements of the local chiral-odd operators, Eq. (2.7); both calculations give identical results. Our numerical results for the isovector and isoscalar tensor charges are

$$\delta u - \delta d = 1.06, \tag{4.8}$$

$$\delta u + \delta d = 0.63. \tag{4.9}$$

These numbers refer to the low normalization point of $\mathcal{O}(600 \text{ MeV})$; however, the scale dependence of these quantities is known to be weak. Our results are consistent with those of previous calculations in the chiral quark-soliton model [47], which were based on a different type of ultraviolet regularization (proper time regularization). Furthermore, we observe a good agreement with the QCD sum rule calculations of Refs. [43,46] and with the lattice estimates of Ref. [44].

Discussion of previous calculations of transversity distributions in the chiral quark-soliton model. The transversity distributions have been computed by Gamberg *et al.* in a description of the nucleon as a chiral soliton of the Nambu–Jona-Lasinio model [42], which is largely equivalent to the chiral quark-soliton model, and by Wakamatsu and Kubota [27] in the same approach as the one used here. In the calculation of Ref. [42] only the contribution of the discrete bound-state level was taken into account. It is known that in general this simplification, which is not warranted by any parametric limit of the model, leads to a number of inconsistencies (e.g., the positivity of the isoscalar unpolarized antiquark distribution is violated), as has been discussed in detail in Refs. [24,25]. In the transversity quark distributions it so happens that the contributions from the Dirac continuum of quarks are numerically small, as shown by the results of our calculation in Fig. 1. In the antiquark distributions, however, the continuum contributions are seen to be numerically important.

In Ref. [27] a calculation of the transversity distribution was presented including also $1/N_c$ corrections to the isovector distribution, $\delta u(x) - \delta d(x)$. As was noted also in Ref. [42], these corrections are afflicted by ordering ambiguities of the collective operators, and it is not clear if the ordering

_____

[5]The flavor asymmetry of the polarized antiquark distributions, $\Delta\bar{u} - \Delta\bar{d}$, was assumed to be zero in most parametrizations, e.g., [3].

adopted in Ref. [27] is correct. Short of a satisfactory answer to these questions we have chosen to limit ourselves to the contributions appearing in the lowest nonvanishing order of $1/N_c$. A detailed investigation of the $1/N_c$ corrections will be reported elsewhere.

An important difference of our results to those of Ref. [27] concerns the ultraviolet regularization. In Ref. [27] the Dirac continuum contributions to all distributions was subjected to a Pauli-Villars subtraction, although our analysis shows that these quantities are ultraviolet finite and do not require regularization. In contrast, we have left these distributions unregularized. A more detailed comparison with the results of Ref. [27] is, unfortunately, not possible, since it is not clear how the anomaly-type phenomenon discovered in our calculation (see Sec. III E) affects the results of Ref. [27], where the equivalence of the summation over occupied and nonoccupied levels in the final results was not convincingly established.

C. Inequalities in the large-N_c limit

The formal limit of large N_c allows one to derive certain positivity bounds for the transversity distributions, as well as generalizations of the Soffer inequalities, which are stronger than those which hold in QCD at $N_c = 3$ [40]. It is interesting to check if these inequalities are satisfied by the results of the numerical calculations.

In Ref. [34] the following positivity constraints were derived in the large-N_c limit of QCD:

$$\frac{u(x)+d(x)}{3} \geq |\Delta u(x) - \Delta d(x)|, \qquad (4.10)$$

$$\frac{u(x)+d(x)}{3} \geq |\delta u(x) - \delta d(x)|, \qquad (4.11)$$

and similarly for the corresponding antiquark distributions. In the chiral quark-soliton model the second inequality is trivially satisfied in the limit of large ultraviolet cutoff, since the isoscalar unpolarized distribution is logarithmically divergent, while the transversity distributions are finite. For finite cutoff, however, the inequalities could in principle be violated by the ultraviolet regularization. In Fig. 4 we have plotted the results for both the LHS and RHS in the chiral quark-soliton model. (The isoscalar unpolarized distribution has been taken from Ref. [56].) One sees that the numerical results respect the inequalities, for both the quark and antiquark distributions, to a very good extent. The small numerical violation should be attributed to the ultraviolet regularization. It is interesting that for the quarks we observe saturation of the inequality for the transversity distribution, while the longitudinally polarized distribution is smaller than its bound, while for antiquarks the situation is opposite: The longitudinally polarized distribution saturates the inequality, and the transversity distribution falls short of its bound. This qualitative behavior could be a useful guideline for parametrizing the distributions in analysis of experimental data.
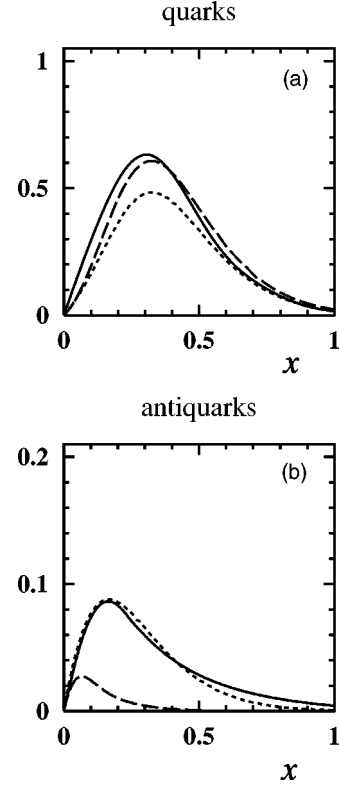

FIG. 4. The large-N_c improved positivity bounds for quark distribution functions, Eqs. (4.10) and (4.11), for the quark (left) and antiquark distributions (right). Solid lines: $x[u+d](x)/3$. Dashed lines: $|x[\delta u - \delta d](x)|$. Dotted lines: $x[\Delta u - \Delta d](x)$.

Similar is the situation with the "large-N_c version" of the Soffer inequalities. In Ref. [40] the following large-N_c inequalities were proved:

$$\frac{1}{2}\left[\frac{u(x)+d(x)}{3} + (\Delta u(x) - \Delta d(x))\right] \geq |\delta u(x) - \delta d(x)|. \qquad (4.12)$$

In Fig. 5 we plot the LHS and RHS of this inequality, as obtained in the model calculation in the large-N_c limit. The same caveats concerning the ultraviolet regularization apply as in the case of the positivity conditions discussed above. As we can see, the model results satisfy the inequality within the expected accuracy.

V. TRANSVERSE SPIN ASYMMETRIES IN POLARIZED DRELL-YAN PAIR PRODUCTION

With the numerical results for the transversity quark and antiquark distributions we can proceed to make predictions for observables which would allow us to extract these distributions from experiment. As explained in the Introduction, the transversity distributions cannot be measured in inclusive DIS at leading-twist level. In semi-inclusive DIS they enter together with chirally odd fragmentation functions, which, too, are essentially unknown quantities [1]. The cleanest way to measure the transversity distribution at leading-twist level seems to be Drell-Yan (DY) pair production in scattering of
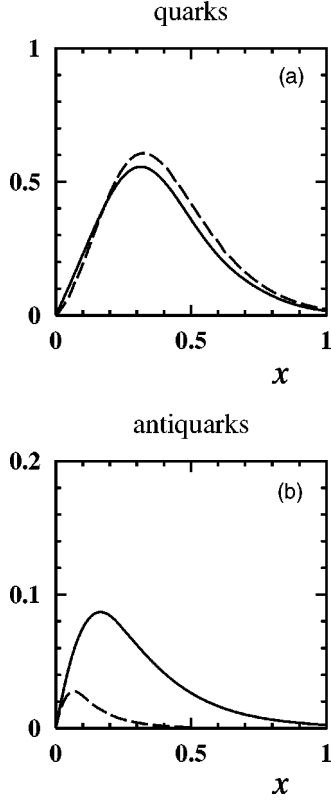
quarks

antiquarks

FIG. 5. The large-N_c improved Soffer bound for the quark (left) and antiquark (right) distributions. Dashed lines: $|x[\delta u - \delta d](x)|$. Solid lines: the large-N_c Soffer bound $\{x[u+d](x)/3 + x[\Delta u - \Delta d](x)\}/2$. The small violation is due to the ultraviolet regularization; see the discussion in the main text.

transversely polarized pp or $p\bar{p}$. We shall therefore concentrate on this process here.

The cross section for DY pair production is a function of the center-of-mass energy of the incoming protons, $s = (p_1 + p_2)^2$, and of the invariant mass of the produced lepton pair, $M^2 = (k_1 + k_2)^2$, which is equal to the virtuality of the exchanged photon and where $k_{1/2}$ are the momenta of the detected leptons. At the partonic level this process is described by the annihilation of a quark and an antiquark originating from the two protons, carrying, respectively, longitudinal momenta $x_1 p_1$ and $x_2 p_2$.[6] The momentum fractions are given by $x_{1/2} = (Q^2/s)^{1/2} e^{\pm y}$ with rapidity $y = \frac{1}{2}\ln[p_1(k_1 + k_2)/p_2(k_1 + k_2)]$. We consider the case that the two protons are transversely polarized relative to the beam direction. In leading-order QCD the transverse spin asymmetry of the DY cross section is given by

$$A_{TT}^{pp}(y;s,M^2) = \frac{\sum_f e_f^2 \delta q_f(x_1,M^2)\, \delta q_{\bar{f}}(x_2,M^2)}{\sum_f e_f^2 q_f(x_1,M^2)\, q_{\bar{f}}(x_2,M^2)}, \quad (5.1)$$

---

[6]For questions concerning the reconstruction of the partonic initial state from the event data, see, e.g., Refs. [60,61].

where the sum runs over all species of light quarks and antiquarks in the two nucleons, $f = \{u,\bar{u},d,\bar{d},\dots\}$. The relevant scale here for the parton distribution functions is the virtuality of the photon, M^2. Note that this asymmetry is sensitive to the antiquark distributions. We neglect strange quark contributions here; since they always enter in the form of a product of a strange quark with a strange antiquark distribution, they can be expected to be very small.

In the case of DY pair production in $p\bar{p}$ rather than pp collisions, using charge conjugation $\delta q_{f/p}(x) \equiv \delta q_{\bar{f}/\bar{p}}(x)$ and $q_{f/p}(x) \equiv q_{\bar{f}/\bar{p}}(x)$, the above expression changes to

$$A_{TT}^{p\bar{p}}(y;s,M^2) = \frac{\sum_f e_f^2 \delta q_f(x_1,M^2)\, \delta q_f(x_2,M^2)}{\sum_f e_f^2 q_f(x_1,M^2)\, q_f(x_2,M^2)}. \quad (5.2)$$

The transverse spin asymmetry, Eqs. (5.1) and (5.2), requires the quark and antiquark distributions of the individual quark flavors $\delta u(x)$, $\delta d(x)$, $\delta\bar{u}(x)$, and $\delta\bar{d}(x)$. In our approach, based on the large-N_c limit, we have computed the isovector distribution $[\delta u(x) - \delta d(x), \delta\bar{u}(x) - \delta\bar{d}(x)]$, which appears in leading order of the $1/N_c$ expansion, and the isoscalar $[\delta u(x) + \delta d(x), \delta\bar{u}(x) + \delta\bar{d}(x)]$, which appears in next-to-leading order, both in the lowest nonvanishing order of $1/N_c$. From these results one should not, strictly speaking, recover the distribution of the individual flavors by adding and subtracting the isovector and isosinglet combination, since there can be $1/N_c$ corrections to the isovector distribution, of the same order in $1/N_c$ as the isosinglet distribution, which are not included. Such $1/N_c$ corrections were studied in Ref. [27]; however, we did not compute them here but rather take a pragmatic stand. We directly reconstruct the individual flavor distributions from the results of the model calculations. For the quark transversity distributions we take the model result for the ratios of transversity to longitudinally polarized distributions, Eqs. (4.6) and (4.7), together with the Glück-Reya-Stratmann-Vogelsang 1995 (GRSV 95) LO distribution for the longitudinally polarized distributions. For the antiquark transversity distributions we neglect the contribution of the isoscalar distribution as it is much smaller than the isovector one (see Figs. 1 and 2).

In order to get an impression of the dependence of the prediction for the transverse spin asymmetries on the choice of transversity distributions we compare the above results with the asymmetries calculated under the assumption that $\delta q(x) \equiv \Delta q(x), \delta\bar{q}(x) \equiv \Delta\bar{q}(x)$, using again the GRSV 95 parametrization for $\Delta q(x)$ and $\Delta\bar{q}(x)$. (This choice, which is consistent with the Soffer inequalities, has frequently been made in the literature [8,62].)

The transverse spin asymmetries obtained with the two "scenarios" for the transversity distributions are shown in Fig. 6 and 7. One sees that the differences in the pp asymmetries are quite sizable, in particular in the region of small rapidities. Note, however, that these observables depend very sensitively on the small antiquark distributions, which may be affected by $1/N_c$ corrections. Even greater differences are
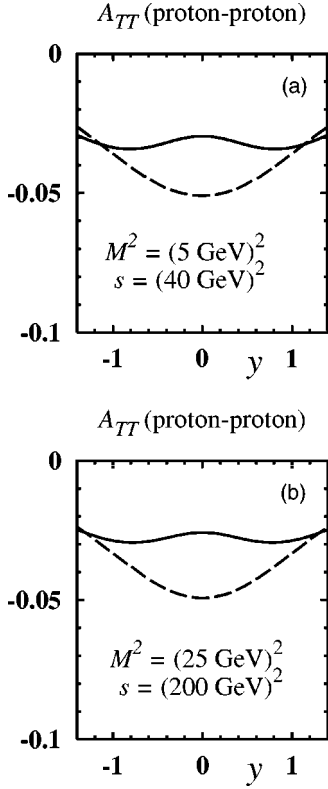
FIG. 6. The transverse spin asymmetry A_{TT}, Eq. (5.1), in collisions of transversely polarized protons, in two different kinematical regions: $s=(40\ \text{GeV})^2$, $M^2=(5\ \text{GeV})^2$ (left) and $s=(500\ \text{GeV})^2$, $M^2=(25\ \text{GeV})^2$ (right). Solid lines: asymmetries calculated with the quark and antiquark distributions computed in the chiral quark-soliton model; cf. Fig. 2. For the quark distributions we used the calculated ratios of transversity to longitudinally polarized distributions, Eqs. (4.6) and (4.7), together with the GRSV 95 parametrizations [3] for $[\Delta u-\Delta d](x)$ and $[\Delta u+\Delta d](x)$. Dashed lines: asymmetries obtained assuming that $\delta q(x)\equiv\Delta q(x)$ and $\delta\bar{q}(x)\equiv\Delta\bar{q}(x)$ ($q=u,d$), using the GRSV 95 parametrizations [3] for $\Delta q(x)$ and $\Delta\bar{q}(x)$.

FIG. 7. The transverse spin asymmetry $A_{TT}^{p\bar{p}}$, Eq. (5.2), in collisions of transversely polarized protons and antiprotons. The solid and dashed lines correspond to the cases described in Fig. 6.

seen in the asymmetries for $p\bar{p}$ reactions. Here the asymmetries are dominated by the products of quark distributions in the proton, while the contributions from the antiquark distributions are negligible. The differences between the asymmetries calculated with our model distributions and those with $\delta q(x)\equiv\Delta q(x)$ essentially reflect the numerical enhancement of the transversity quark distributions over the longitudinally polarized ones found in the model calculations; cf. Eqs. (4.6) and (4.7). To summarize, we find that our model distributions result in significant deviations from what is obtained with that approximation [63–65]. Unfortunately, recent studies, taking into account the limited detector acceptance, suggest that measurements at RHIC are unlikely to be able to discriminate between the two scenarios [66].

VI. CONCLUSIONS

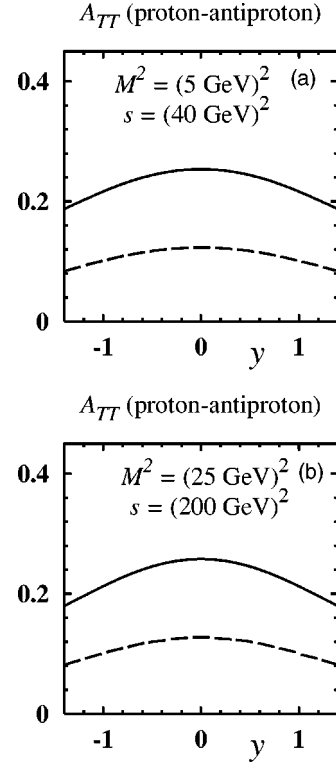In this paper we have studied the transversity quark and antiquark distributions in a dynamical model of the nucleon

based on the large-N_c limit. Let us briefly summarize the main qualitative conclusions.

Comparing the transversity and longitudinally polarized distributions, we found that, generally speaking, the quark distributions (both isovector and isoscalar) are comparable in magnitude. The corresponding antiquark distributions, on the contrary, are very different. Appealing to the gradient expansion, which, as we saw, gives a realistic numerical description of the antiquark distributions, we were able to explain the smallness of the isovector transversity antiquark distribution relative to its longitudinally polarized counterpart on grounds of the constraints imposed on the low-energy effective dynamics by chiral symmetry. A measurement of the transversity antiquark distributions would thus be a sensitive test of the role of chiral symmetry in determining the parton distributions of the nucleon at a low scale.[7]

The strong differences between the longitudinally and transversity antiquark distributions should be taken into ac-

———

[7]Also, it would be interesting to see if the the differences between the longitudinally and transversity antiquark distributions can qualitatively be understood in the popular ''pion cloud'' picture, which is widely used to explain the flavor asymmetry of the unpolarized antiquark distributions, $\bar{u}-\bar{d}$. We stress that that model is not related to the large-N_c approach employed in this work; see Refs. [32,67] for a critical discussion. The issue of polarization of the antiquark distributions in the ''pion cloud'' model has recently been discussed in Ref. [32].

count when making predictions for observables sensitive to the antiquark distributions. Our estimates show that these differences have a noticeable effect, e.g., on the spin asymmetries in polarized Drell-Yan pair production. It remains to be seen if these asymmetries can be measured to an accuracy that would allow one to discriminate between the different predictions [66].

Also, we have verified that the quark-antiquark distributions obtained in the chiral quark-soliton model satisfy the Soffer inequalities, as well as the large-N_c inequalities derived in Ref. [40]. Since these relations could in principle be violated by the ultraviolet cutoff required in the model calculation, their fulfillment should be seen as another piece of evidence in favor of the Pauli-Villars regularization scheme adopted here [24,25,56].

We have noted a curious anomaly-type phenomenon in the tensor charge and the transversity distribution functions. Here we have described this phenomenon using the language of sums over quark single-particle levels in the background pion field specific to our large-N_c picture of the nucleon. It is possible, however, that the anomaly described here has meaning also outside of the context of this model. To clarify this one should see if the observations made here could be stated in a more general, field-theoretic language. The analogy with the Fujikawa formulation of the U(1) anomaly [57], whose field-theoretical description is well known, should be a useful guideline.

APPENDIX: ANOMALY-TYPE PHENOMENON IN THE TRANSVERSITY DISTRIBUTION FUNCTION

In the calculation of the isovector transversity distribution function in the effective chiral theory we encounter an anomaly-type phenomenon: The distributions obtained by summing the contributions of occupied and nonoccupied quark levels in the soliton are different if the soliton field does not fall off faster than $1/r^2$ at large distances. In Sec. III E we computed the anomalous difference in the first moment of the isovector distribution, i.e., the isovector tensor charge. Using a somewhat different approach one can easily compute the anomalous difference in the x-dependent distribution function. Since the anomaly phenomenon in the transversity distribution is of principal theoretical interest, as well as of practical importance for the numerical calculations (see Sec. IV B), we derive here the expression for the anomalous difference of the isovector distribution function.

The representation of the isovector transversity distribution as a sum over occupied quark levels, Eq. (3.37), can be

written as an integral over a continuous energy variable ω in the form[8]

$$[\delta u(x) - \delta d(x)]_{\text{occup}} = \int_{-\infty}^{E_{lev}+0} d\omega \, \rho(\omega), \qquad \text{(A1)}$$

where the integrand $\rho(\omega)$ is defined by the functional trace of the quark "density of states," $\delta(\omega - H)$, with the relevant single-particle operator

$$\rho(\omega) \equiv \frac{2N_c M_N}{3} \text{Sp}\left[\delta(\omega - H)\delta(\omega + P^3 - xM_N) \right.$$
$$\left. \times \frac{1+\gamma^0\gamma^3}{2}\gamma^5\gamma^1\tau^1 \right]. \qquad \text{(A2)}$$

Here, P^i denotes the single-particle three-momentum operator and H the Dirac Hamiltonian, Eq. (3.5). Similarly, the representation of the distribution as a sum over nonoccupied quark levels, Eq. (3.38), can be written in the form

$$[\delta u(x) - \delta d(x)]_{\text{nonoccup}} = -\int_{E_{lev}+0}^{\infty} d\omega \, \rho(\omega). \qquad \text{(A3)}$$

The difference between the two representations is thus given as an integral over *all* energies:

$$[\delta u(x) - \delta d(x)]_{\text{occup}} - [\delta u(x) - \delta d(x)]_{\text{nonoccup}}$$
$$= \int_{-\omega_0}^{\omega_0} d\omega \, \rho(\omega). \qquad \text{(A4)}$$

We have introduced here an explicit energy cutoff ω_0 in order to specify the limiting procedure leading to the anomaly. In order to analyze the difference, Eq. (A4), in the limit of large ω_0 we write the delta function of $\omega - H$ as the imaginary part of the quark propagator [25]:

$$[\delta u(x) - \delta d(x)]_{\text{occup}} - [\delta u(x) - \delta d(x)]_{\text{nonoccup}}$$
$$= \frac{4N_c M_N}{3}\text{Im}\int_{-\omega_0}^{\omega_0}\frac{d\omega}{2\pi}\text{Sp}\left[\frac{1}{H-\omega-i0}\delta(\omega + P^3 - xM_N)\right.$$
$$\left. \times\frac{1+\gamma^0\gamma^3}{2}\gamma_5\gamma^1\tau^1\right]. \qquad \text{(A5)}$$

We now proceed as in the case of the tensor charge in Sec. III E, and expand the integrand for large ω. This can be done by writing the quark propagator in the form

$$\frac{1}{H-\omega-i0} = \frac{H+\omega}{H^2-\omega^2-i0\,\text{sgn}\,\omega}, \qquad \text{(A6)}$$

and substituting the formal series expansion of this expression in powers of derivatives of the pion field, Eq. (3.50),

---

[8]Throughout this section it will be understood that $\delta u(x)$, etc., denotes the quark distribution for $x>0$ and minus the antiquark distribution at $x<0$; cf. Eq. (2.5).

collecting all terms contributing in a certain order of $1/\omega$. In our case the leading contribution in $1/\omega$ comes from term with $n=1$ in Eq. (3.50); the term with $n=0$ cannot produce a γ^1 Dirac matrix needed to compensate the γ^1 matrix in the operator in Eq. (A5). Taking into account also γ_5 parity one finds that the leading contribution at large ω is given by

$$
[\delta u(x) - \delta d(x)]_{\text{occup}} - [\delta u(x) - \delta d(x)]_{\text{nonoccup}} = \frac{4N_c M_N}{3} \text{Im} \int_{-\omega_0}^{\omega_0} \frac{d\omega}{2\pi} \text{Sp} \left\{ \frac{(\omega - i\gamma^0 \gamma^k \partial_k)}{[-\partial^2 + M^2 - \omega^2 - i0 \, \text{sgn} \, \omega]^2} \delta(\omega + P^3) \right.
$$

$$
\left. - x M_N) \frac{1 + \gamma^0 \gamma^3}{2} \gamma_5 \gamma^1 \tau^1 [-iM(\gamma^k \partial_k U_{\text{cl}}^{\gamma_5})] \right\}.
\tag{A7}
$$

We can evaluate the functional trace in the basis of momentum eigenstates, $\text{Sp}[\cdots] = \int d^3 p (2\pi)^3 \langle p | \cdots | p \rangle$, inserting complete sets of intermediate position eigenstates in which the pion field is diagonal. In addition, we have to take the trace over Dirac and flavor indices. In this way we obtain

$$
[\delta u(x) - \delta d(x)]_{\text{occup}} - [\delta u(x) - \delta d(x)]_{\text{nonoccup}}
$$

$$
= \frac{4N_c M_N}{3} \text{Im} \int_{-\omega_0}^{\omega_0} \frac{d\omega}{2\pi} \int \frac{d^3 p}{(2\pi)^3} \text{Tr}_{\text{Dirac}} \left\{ \frac{(\omega + \gamma^0 \gamma^k p^k) \delta(\omega + p^3 - x M_N)}{[|\mathbf{p}|^2 + M^2 - \omega^2 - i0 \, \text{sgn} \, \omega]^2} \frac{1 + \gamma^0 \gamma^3}{2} \gamma_5 \gamma^1 \right.
$$

$$
\left. \times \int d^3 x \, \text{Tr}_{\text{flavor}}[-iM \gamma^k \partial_k U_{\text{cl}}^{\gamma_5}(\mathbf{x}) \tau^1] \right\}
\tag{A8}
$$

$$
= \frac{16 N_c M_N M}{3} \int d^3 x \, \text{Tr}_{\text{flavor}} \{ i \tau^1 \partial_1 [U_{\text{cl}}(\mathbf{x}) - U_{\text{cl}}^\dagger(\mathbf{x})] \} \text{Im} \int_{-\omega_0}^{\omega_0} \frac{d\omega}{2\pi} \int \frac{d^3 p}{(2\pi)^3} \frac{(\omega + p^3) \delta(\omega + p^3 - x M_N)}{[|\mathbf{p}|^2 + M^2 - \omega^2 - i0 \, \text{sgn} \, \omega]^2}.
\tag{A9}
$$

It remains to compute the integral over the energy ω and the momentum p in the last expression. Instead of computing the integral first and then taking its imaginary part it is convenient to take the imaginary part "under the integral," substituting

$$
\text{Im} \left[(\omega + p^3) \delta(\omega + p^3 - x M_N) \frac{1}{(|\mathbf{p}|^2 + \mathbf{M}^2 - \omega^2 - i0 \, \text{sgn} \, \omega)^2} \right]
$$

$$
\to (\omega + p^3) \delta(\omega + p^3 - x M_N) \pi(-\text{sgn} \, \omega)
$$

$$
\times \delta'(|\mathbf{p}|^2 + \mathbf{M}^2 - \omega^2)
$$

$$
= x M_N \delta(\omega + p^3 - x M_N) \pi(-\text{sgn} \, \omega)
$$

$$
\times \delta'[-x M_N(\omega - p^3) + |\mathbf{p}^\perp|^2 + M^2].
\tag{A10}
$$

In the last step here we have made use of the condition imposed by the first delta function in order to simplify the integrand. The integral over p^3 can be taken using up the first delta function:

$$
\int_{-\omega_0}^{\omega_0} \frac{d\omega}{2\pi} \int \frac{d^3 p}{(2\pi)^3} \text{Im}[\cdots]
$$

$$
= \int_{-\omega_0}^{\omega_0} \frac{d\omega}{2\pi} \int \frac{d^2 p^\perp}{(2\pi)^2} x M_N(-\text{sgn} \, \omega)
$$

$$
\times \delta'[-x M_N(2\omega - x M_N) + |\mathbf{p}^\perp|^2 + M^2].
\tag{A11}
$$

The integral over ω requires some care. We have

$$
\int_{-\omega_0}^{\omega_0} \frac{d\omega}{2\pi} (-\text{sgn} \, \omega) \delta'[-x M_N(2\omega - x M_N) + |\mathbf{p}^\perp|^2 + \mathbf{M}^2]
$$

$$
= \left(-\int_0^{\omega_0} + \int_{-\omega_0}^0 \right) \frac{d\omega}{2\pi} \delta'[-x M_N(2\omega - x M_N)
$$

$$
+ |\mathbf{p}^\perp|^2 + \mathbf{M}^2]
\tag{A12}
$$

$$
= \frac{1}{2 x M_N} \frac{1}{2\pi} \delta[-x M_N(2\omega_0 - x M_N)
$$

$$
+ |\mathbf{p}^\perp|^2 + \mathbf{M}^2] + (\omega_0 \to -\omega_0).
\tag{A13}
$$

The remaining integral over the transverse component of p can easily be performed after replacing

$$
\int \frac{d^2 p^\perp}{(2\pi)^2} \to \int \frac{d|\mathbf{p}^\perp|^2}{4\pi}.
$$

It gives rise to a sum of two step functions, which in the limit of large cutoff, $\omega_0 \to \infty$, are nonzero for values of x in the range

$$
-2\omega_0/M_N < x < 2\omega_0/M_N.
\tag{A14}
$$

Collecting everything we obtain, from Eq. (A9),

$$[\delta u(x) - \delta d(x)]_{\text{occup}} - [\delta u(x) - \delta d(x)]_{\text{nonoccup}}$$

$$= \frac{N_c M_N M}{6\pi^2} \theta\left(\frac{-2\omega_0}{M_N} < x < \frac{2\omega_0}{M_N}\right)$$

$$\times \int d^3x \, \text{Tr}_{\text{flavor}}[i\tau^1 \partial_1(U_{\text{cl}} - U_{\text{cl}}^\dagger)]. \qquad (A15)$$

Equation (A15) represents the result for the ''anomalous difference'' between the sums over occupied and nonoccupied levels.

As in the case of the tensor charge, Eq. (3.57), the anomalous difference of the distribution functions, Eqs. (A15), is given by a total derivative of the pion field, which is nonzero only if the field drops like $1/r^2$ at large distances, $r \to \infty$. In this case the unitary matrix at large r takes the form

$$U_{\text{cl}} = 1 + \frac{\kappa}{r^2} i(n^k \tau^k), \qquad (A16)$$

where the constant κ is related to the nucleon isovector axial coupling constant in the chiral limit by Eq. (3.56). The integral of the total derivative of the pion field then becomes[9]

$$\int d^3x \, \text{Tr}_{\text{flavor}}[i\tau^1 \partial_1(U_{\text{cl}} - U_{\text{cl}}^\dagger)]$$

$$= \frac{1}{3} \int d^3x \, \text{Tr}_{\text{flavor}}\left[\sum_{k=1}^{3} i\tau^k \partial_k(U_{\text{cl}} - U_{\text{cl}}^\dagger)\right]$$

$$= \lim_{r \to \infty} \frac{4\pi r^2}{3} \text{Tr}_{\text{flavor}}\left[i\sum_{k=1}^{3} n^k \tau^k(U_{\text{cl}} - U_{\text{cl}}^\dagger)\right]$$

_____

[9]Instead of converting the integral of the total derivative of the pion field into a surface integral at $r = \infty$, one also may directly differentiate the asymptotic form of the pion field, Eq. (A16), and compute the volume integral. In this case one would find that the derivative of the $1/r^2$ term in Eq. (A16) gives rise to a delta function at $r = 0$, whose volume integral reproduces Eq. (A17).

$$= -\frac{4\pi\kappa}{3} = \frac{2g_A}{9F_\pi^2}. \qquad (A17)$$

The anomalous difference is thus given by

$$[\delta u(x) - \delta d(x)]_{\text{occup}} - [\delta u(x) - \delta d(x)]_{\text{nonoccup}}$$

$$= \frac{1}{12\pi^2} \frac{g_A}{F_\pi^2} N_c M_N M \, \theta\left(-\frac{2\omega_0}{M_N} < x < \frac{2\omega_0}{M_N}\right).$$

$$(A18)$$

The support of this function increases with the energy cutoff ω_0. A similar phenomenon was observed in the anomalous difference in the isoscalar unpolarized distribution in Ref. [25]. The moments of this function (with respect to the variable x) thus exhibit power divergences for $\omega_0 \to \infty$. In particular, the first moment is linearly divergent[10]:

$$\int_{-\infty}^{\infty} dx \{[\delta u(x) - \delta d(x)]_{\text{occup}} - [\delta u(x) - \delta d(x)]_{\text{nonoccup}}\}$$

$$= \frac{N_c M g_A \omega_0}{3\pi^2 F_\pi^2}. \qquad (A19)$$

This is in qualitative agreement with the behavior of the tensor charge in the limit of large energy cutoff derived in Sec. III E. Note that the coefficient of the linear divergence depends on the details of the ultraviolet cutoff used, so one should not expect to find the same coefficients in Eqs. (A19) and (3.57).

_____

[10]In the large-N_c limit the support of the parton distributions is not limited to the $-1 < x < 1$, so we must integrate over the entire real axis in order to recover the tensor charge as defined by the matrix element of the local operator, Eq. (2.7).

---

[1] R.L. Jaffe, in Proceedings of ''Deep inelastic scattering off polarized targets, Physics with polarized protons at HERA,'' Hamburg/Zeuthen, 1997, pp. 167–180, Report No. MIT-CTP-2685, hep-ph/9710465.

[2] J.P. Ralston and D.E. Soper, Nucl. Phys. **B152**, 109 (1979).

[3] M. Glück, E. Reya, M. Stratmann, and W. Vogelsang, Phys. Rev. D **53**, 4775 (1996).

[4] M. Glück, E. Reya, and A. Vogt, Z. Phys. C **67**, 433 (1995).

[5] A.D. Martin, R.G. Roberts, W.J. Stirling, and R.S. Thorne, Eur. Phys. J. C **4**, 463 (1998).

[6] CTEQ Collaboration, H.L. Lai, J. Huston, S. Kuhlmann, J. Morfin, F. Olness, J.F. Owens, J. Pumplin, and W.K. Tung, Eur. Phys. J. C **12**, 375 (2000).

[7] R.L. Jaffe and X.-D. Ji, Phys. Rev. Lett. **67**, 552 (1991); Nucl. Phys. **B375**, 527 (1992).

[8] X.-D. Ji, Phys. Lett. B **284**, 137 (1992).

[9] R.L. Jaffe and N. Saito, Phys. Lett. B **382**, 165 (1996).

[10] J. Collins, Nucl. Phys. **B396**, 161 (1993); X. Artru and J. Collins, Z. Phys. C **69**, 277 (1996).

[11] A.M. Kotzinian and P.J. Mulders, Phys. Lett. B **406**, 373 (1997).

[12] D. Boer and P.J. Mulders, Phys. Rev. D **57**, 5780 (1998); D. Boer, R. Jakob, and P.J. Mulders, Phys. Lett. B **424**, 143 (1998); D. Boer and R. Tangerman, *ibid.* **381**, 305 (1996); P.J. Mulders and R. Tangerman, Nucl. Phys. **B461**, 234 (1995).

[13] A.V. Efremov, hep-ph/0001214.

[14] V.A. Korotkov, W.D. Nowak, and K.A. Oganesian, Eur. Phys. J. C **18**, 639 (2001)

[15] A.M. Kotzinian, K.A. Oganesian, H.R. Avakian, and E. De Sanctis, hep-ph/9908466.

[16] M. Boglione and P.J. Mulders, Phys. Lett. B **478**, 114 (2000).

[17] A.V. Efremov, K. Goeke, M.V. Polyakov, and D. Urbano, Phys. Lett. B **478**, 94 (2000).

[18] HERMES Collaboration, H. Avakian, Nucl. Phys. B (Proc. Suppl.) **79**, 523 (1999); HERMES Collaboration, A. Airapetian *et al.*, Phys. Rev. Lett. **84**, 4047 (2000).

[19] Spin Muon Collaboration, A. Bravar, Nucl. Phys. B (Proc. Suppl.) **79**, 520 (1999).

[20] R.L. Jaffe, X. Jin, and J. Tang, Phys. Rev. Lett. **80**, 1166 (1998); Phys. Rev. D **57**, 5920 (1998).

[21] J. Soffer, Phys. Rev. Lett. **74**, 1292 (1995).

[22] G.R. Goldstein, R.L. Jaffe, and X.-D. Ji, Phys. Rev. D **52**, 5006 (1995).

[23] C. Bourrely, J. Soffer, and O.V. Teryaev, Phys. Lett. B **420**, 375 (1998).

[24] D.I. Diakonov, V.Yu. Petrov, P.V. Pobylitsa, M.V. Polyakov, and C. Weiss, Nucl. Phys. **B480**, 341 (1996).

[25] D.I. Diakonov, V.Yu. Petrov, P.V. Pobylitsa, M.V. Polyakov, and C. Weiss, Phys. Rev. D **56**, 4069 (1997); **58**, 038502 (1998).

[26] D. Diakonov and V. Petrov, Pis'ma Zh. Éksp. Teor. Fiz. **43**, 57 (1986) [JETP Lett. **43**, 75 (1986)]; D. Diakonov, V. Petrov, and P. Pobylitsa, Nucl. Phys. **B306**, 809 (1988).

[27] M. Wakamatsu and T. Kubota, Phys. Rev. D **57**, 5755 (1998); *ibid.* **60**, 034020 (1999).

[28] M. Wakamatsu, Phys. Lett. B **509**, 59 (2001).

[29] P.V. Pobylitsa, M.V. Polyakov, K. Goeke, T. Watabe, and C. Weiss, Phys. Rev. D **59**, 034024 (1999).

[30] For a more detailed discussion of the flavor asymmetries, see B. Dressler, K. Goeke, P.V. Pobylitsa, M.V. Polyakov, T. Watabe, and C. Weiss, in Proceedings of the 11th International Conference on Problems of Quantum Field Theory, Dubna, Russia, 1998, hep-ph/9809487.

[31] M. Wakamatsu and T. Watabe, Phys. Rev. D **62**, 054009 (2000).

[32] B. Dressler, K. Goeke, M.V. Polyakov, and C. Weiss, Eur. Phys. J. C **14**, 147 (2000).

[33] B. Dressler, K. Goeke, M.V. Polyakov, P. Schweitzer, M. Strikman, and C. Weiss, Eur. Phys. J. C **18**, 719 (2001).

[34] P.V. Pobylitsa and M.V. Polyakov, Phys. Lett. B **389**, 350 (1996).

[35] V.Yu. Petrov, P.V. Pobylitsa, M.V. Polyakov, I. Börnig, K. Goeke, and C. Weiss, Phys. Rev. D **57**, 4325 (1998).

[36] For a review, see Ch.V. Christov *et al.*, Prog. Part. Nucl. Phys. **37**, 91 (1996).

[37] R. Alkofer, H. Reinhardt, and H. Weigel, Phys. Rep. **265**, 139 (1996).

[38] K. Goeke, P.V. Pobylitsa, M.V. Polyakov, and D. Urbano, Nucl. Phys. **A680**, 307 (2000).

[39] K. Goeke, P.V. Pobylitsa, M.V. Polyakov, P. Schweitzer, and D. Urbano, Acta Phys. Pol. B **32**, 1201 (2001).

[40] P.V. Pobylitsa and M.V. Polyakov, Phys. Rev. D **62**, 097502 (2000).

[41] S. Scopetta and V. Vento, Phys. Lett. B **424**, 25 (1998).

[42] L. Gamberg, H. Reinhardt, and H. Weigel, Phys. Rev. D **58**, 054014 (1998).

[43] B.L. Ioffe and A. Khodjamirian, Phys. Rev. D **51**, 3373 (1995).

[44] S. Aoki, M. Doui, T. Hatsuda and Y. Kuramashi, Phys. Rev. D **56**, 433 (1997).

[45] Y. Kuramashi, Nucl. Phys. **A629**, 235C (1998).

[46] H. He and X. Ji, Phys. Rev. D **54**, 6897 (1996).

[47] H. Kim, M.V. Polyakov, and K. Goeke, Phys. Rev. D **53**, 4715 (1996); Phys. Lett. B **387**, 577 (1996).

[48] X. Artru and M. Mekhfi, Z. Phys. C **45**, 669 (1990).

[49] W. Vogelsang, Phys. Rev. D **57**, 1886 (1998).

[50] A. Hayashigaki, Y. Kanazawa, and Y. Koike, Phys. Rev. D **56**, 7350 (1997).

[51] E. Witten, Nucl. Phys. **B223**, 433 (1983).

[52] D. Diakonov and V. Petrov, Nucl. Phys. **B245**, 259 (1984); **B272**, 457 (1986); LNPI Report No. LNPI-1153, 1986, published (in Russian) in Hadron Matter under Extreme Conditions, Naukova Dumka, Kiev, 1986, p. 192.

[53] D. Diakonov and M. Eides, Pis'ma Zh. Éksp. Teor. Fiz. **38**, 358 (1983) [JETP Lett. **38**, 433 (1983)]; A. Dhar, R. Shankar, and S. Wadia, Phys. Rev. D **31**, 3256 (1985).

[54] G. Adkins, C. Nappi, and E. Witten, Nucl. Phys. **B228**, 552 (1983).

[55] J. Balla, M.V. Polyakov, and C. Weiss, Nucl. Phys. **B510**, 327 (1997).

[56] C. Weiss and K. Goeke, Bochum University Report No. RUB-TPII-12/97, hep-ph/9712447.

[57] K. Fujikawa, Phys. Rev. D **21**, 2848 (1980).

[58] M. Praszałowicz, A. Blotz, and K. Goeke, Phys. Lett. B **354**, 415 (1995).

[59] S. Kahana and G. Ripka, Nucl. Phys. **A429**, 462 (1984).

[60] G. Bunce *et al.*, Part. World **3**, 1 (1992); PHENIX/Spin Collaboration, "Spin Structure Function Physics with an upgraded PHENIX Muon Spectrometer," 1994 (unpublished), available at http://www.rhic.bnl.gov/phenix.

[61] G. Bunce, N. Saito, J. Soffer, and W. Vogelsang, Annu. Rev. Nucl. Part. Sci. **50**, 525 (2000).

[62] V. Barone, T. Calarco, and A. Drago, Phys. Rev. D **56**, 527 (1997).

[63] C. Bourrely and J. Soffer, Nucl. Phys. **B423**, 329 (1994).

[64] J. Soffer and J.-M. Virey, Phys. Lett. B **314**, 132 (1993); Nucl. Phys. **B509**, 297 (1998).

[65] B. Kamal, Phys. Rev. D **57**, 6663 (1998).

[66] O. Martin, A. Schafer, M. Stratmann, and W. Vogelsang, Phys. Rev. D **60**, 117502 (1999).

[67] W. Koepf, L.L. Frankfurt, and M. Strikman, Phys. Rev. D **53**, 2586 (1996).